

# The expectation value of the number of loops and the left-passage probability in the double-dimer model

Nahid Ghodratipour\* and Shahin Rouhani†

Department of Physics, Sharif University of Technology, P.O. Box 11155-9161, Tehran, Iran

May 18, 2022

## Abstract

We study various statistical properties of the double-dimer model, a generalization of the dimer model, on rectangular domains of the square lattice. We take advantage of the Grassmannian representation of the dimer model, first to calculate the probability distribution of nontrivial loops around a cylinder, which is consistent with the previously known result, and then to calculate the expectation value of the number of loops surrounding two faces and the left-passage probability, both in the discrete and the continuum cases. We also briefly explain the calculation of some related observables. As a by-product, we obtain the partition function of the dimer model in the presence of two and four monomers, and a single monomer on the boundary.

## 1 Introduction

Some recent activities have focused on mathematical theories of critical phenomena, namely Schramm-Loewner Evolution (SLE) and Conformal Loop Ensemble (CLE) [1–8]. SLEs are random planar curves which are characterized by certain conformal invariance property, following a Loewner evolution driven by a Brownian motion with positive diffusivity  $\kappa$  [9–11]. It is a powerful tool in the study of the scaling limits of two-dimensional critical models, which in several cases such as the loop-erased random walk and uniform spanning tree, percolation and the Ising model on specific lattices, the convergence has been established rigorously. CLEs are ensembles of countably random collection of planar conformally invariant non-crossing and non-self-crossing loops in simply connected domains of the complex plane, indexed by a parameter  $\kappa$  in  $(8/3, 8]$  and constructed by branching variants of SLEs [7]. Both ideas are interesting to physicists because they are related to interfaces in critical phenomena, where early attentions to SLE were mainly motivated by Smirnov’s proof of Cardy’s formula, which in turn leads to the convergence of the percolation exploration path to the chordal SLE<sub>6</sub>. Further the scaling limit of the Ising model was proved to be SLE<sub>3</sub> or SLE<sub>16/3</sub>, determined by the representation [12, 13]. Alternatively, it is related to a conformally invariant loop model at criticality hence a CLE, with either  $\kappa = 3$  or  $\kappa = 16/3$ .

Loop models are among most important and richest classes of two-dimensional statistical lattice models and indeed, many statistical mechanical models are best understood in terms of random paths, open or closed, at criticality [14–16]. In addition to providing geometrical explanations and tools, it employs many methods to study scaling limits, including Coulomb gas formalism [17], Conformal Field Theory (CFT) [18] and more recently, rigorous theories such as SLE and CLE [19, 20]. In all these theories conformal invariance plays a crucial role, enables them to determine critical exponents and other associated universal properties of two-dimensional critical systems such as correlation functions exactly. SLEs (CLEs) are believed to be the scaling limits of various random loop models from

---

\*ghodratipour\_n@physics.sharif.edu

†srouhani@sharif.ir

statistical physics, including the  $O(n)$  models. These are a large class of critical systems in physics, conjectured to be related to  $SLE_\kappa$  and  $CLE_\kappa$  concisely expressed by the formula  $n = -2 \cos(4\pi/\kappa)$ . The parameter  $\kappa$  is so in significant relation to the central charge  $c$  in CFT and as a fact, SLEs (CLEs) with  $\kappa \leq 4$  are believed to be the minimal models of CFT with  $c$  in  $[0, 1]$  [21–23]. One prototypical model where such issues are concerned is the two-dimensional Gaussian Free Field (GFF).

The two-dimensional GFF is a central object both in physics and mathematics, related to the Coulomb gas, which falls into the same universality class as other statistical mechanical models such as the XY-model and the two-dimensional sine-Gordon model [17, 24, 25]. It is the mathematical model of two-dimensional bosonic CFT, and is a two-dimensional analog of the Brownian motion [26]. The notions associated with the Brownian motion, such as the Gaussian measure, the Laplacian, the Green’s function and consequently conformal invariance, are also substantial in GFF [25, 27], and many stochastic differential equations in two dimensions depend on it as those in one dimension on the Brownian motion [28, 29]. We can practically think of GFF as a natural model of random height functions though it is actually a generalized function or a distribution (in sense of Schwartz [26]). It yields a dual interpretation of many loop models, especially the  $O(n)$  models, which in SLE/CLE formalism, is very natural in the case of  $\kappa = 4$  (equivalently  $n = 2$ ); the zero level line of the Gaussian free field (with appropriate boundary conditions) is a chordal  $SLE_4$  and the collection of level loops of it corresponds to  $CLE_4$  [30, 31].

Besides, there is a family of conformally invariant loop models in two dimensions, the Brownian Loop Soups (BLSs), which is deeply related to SLE and CLE [20, 32]. Each BLS is a Poisson point process of Brownian loops [33], with intensity parameter related to  $\kappa$  via the equation  $c = (3\kappa - 8)(6 - \kappa)/2\kappa$  [32], indicating that for low enough intensities the outer boundaries of clusters of Brownian loops are distributed like CLEs for the spectral parameter between  $8/3$  and  $4$ . This implies that the intensity parameter is the central charge of the relevant CFT for  $c$  in  $[0, 1]$ . Motivated by the relation between BLS, SLE and CLE, a connection between BLS and CFT was discovered analyzing particular expectation values, such as correlation functions of the layering and the winding number operators [34]. The critical BLS ( $c = 1$ ) is closely related to the Gaussian Free Field.

All these relations allow or rather require to exploit achievements of mathematical theories of critical phenomena in physics. In this regard, it is quite standard to find and compute observables in critical lattice models, evidencing and supporting relations to SLE and CLE, and/or determining  $\kappa$ . This is what we have done in this paper, in the case of the double-dimer model. Such efforts are prevalent in statistical physics literature.

The study of relevant SLEs has been performed over the last decade with some degree of success. However, not much work has been done on CLEs by physicists. This is perhaps due to the mathematical tractability of CLEs. To be specific, many two-dimensional physical models result in random surfaces whose contour lines are CLEs, yet in physics literature they are inevitably cut in half and treated as SLEs [35–37].

On the other hand, there are limitations on describing a critical model through SLE. The existence of an SLE curve a priori depends on imposing certain boundary conditions, and many observables, potentially defined on cluster boundaries, could not be supported by SLE. Finding tractable methods of tackling CLE is therefore of importance to the physics community. One way of analyzing CLE is via the double-dimer model which is a straightforward generalization of the dimer model.

The dimer model is the study of canonical measures, i.e. Gibbs measures, on the set of dimer coverings of a graph [25]. A dimer covering or perfect matching of a graph is a collection of occupied edges (dimers) of the graph, such that every vertex is covered exactly once. Dimers can have different fugacities (Boltzmann weights), and the weight of each dimer cover is defined to be the product of all dimer weights in the configuration. Generally, interesting graphs are periodic planar graphs such as the square lattice or the honeycomb lattice.

A double-dimer configuration is a union of two dimer covers, or equivalently a set of even-length simple loops and doubled edges, with the property that every vertex is the endpoint of exactly two edges (which may be doubled) [38]. This immediately leads to a loop model related to CLE; it is interesting to study the properties of the distribution of long loops, especially the conformal invariance of the scaling limit of the “uniform” double-dimer model, and its relation to  $CLE_4/SLE_4$ . The partition function of the double-dimer model is simply the multiplication of partition functions of the two contributing

dimer models, giving a proportionally weight of  $2^k$  to each configuration with  $k$  loops in the uniform case. The double-dimer model offers a tool to study the loop model hence CLE.

Precisely in the case of dimers on a bipartite graph, each configuration can be mapped to a height function, a particular discretization of the GFF [39]. In fact, the scaling limit of the collection of double-dimer loops on a bipartite lattice is proved to be  $\text{CLE}_4$  via this correspondence, whereas in the case of non-bipartite lattices it is still a conjecture.

The dimer model arose initially in physics studying the adsorption of diatomic molecules on a surface [40], later an abstraction and an exact formal solution for planar graphs was proposed by Kasteleyn [41], and independently by Fisher and Temperley [42]. In the case of the square lattice, the exact number of domino-tilings of an  $M \times N$  (both even) surface by  $2 \times 1$  dominos is given by:

$$\mathcal{Q}_0 = \prod_{p=1}^{\frac{M}{2}} \prod_{q=1}^{\frac{N}{2}} \left[ 4 \cos^2 \frac{\pi p}{M+1} + 4 \cos^2 \frac{\pi q}{N+1} \right] \quad (1)$$

which is also the partition function of the dimer model in the uniform case (all dimer fugacities are 1). Since then, corresponding computations have been done for some other lattices (see [43] for a review of various references).

The dimer model is of interest in its own right. While not much practical as a realistic model, the dimer model has inherent interest as an exactly solvable model whose distinguished types of phase transitions can be studied analytically. It has close relation with random matrices and determinantal processes [44–47] and to begin with, the computation of the partition function can be accomplished using determinants [41, 42]. Apart from its connection to many contexts in mathematics, it can be translated to several other statistical mechanical models. There is a correspondence between the two-dimensional Ising model on a graph and the dimer model on a decorated version of this graph [48, 49], makes dimer techniques a supplementary powerful tool to study the Ising model. It also has relations with vertex models [50]. As there are few efficient methods to study the latter, these relations are highly valuable [25, 51].

The fermionic nature of the dimer model, already implied by its relation to the Ising model, is an important feature manifest in Kasteleyn’s Pfaffian solution of the dimer problem. Identically, it exhibits in reformulation of the dimer model in terms of Grassmannian anti-commuting variables, which leads to an exact solution of the close-packed dimer problem on some lattices, especially the square lattice [52]. This method works even when there are some monomers present, results in a more complex exact solution in the case of the boundary monomer-dimer problem, and a formal expression of the partition function in the presence of bulk monomers [53, 54].

The central idea of this paper is to use the fermionic representation of the dimer model to give us a tool for direct study of the CLEs and in fact, to utilize this connection for the exact calculation of certain invariants and correlators.

This paper is organized as follows. In section 2, we review the fermionic representation of the dimer model on the square lattice. We introduce our method, strongly based on [52], and perform the calculation of the partition function of the dimer model on a rectangular domain with free and cylindrical boundary conditions. In section 3, we look at loops around a cylinder and find the distribution of the number of nontrivial loops, which is identical to the previously known result [38]. By approximating the result for a very long cylinder, a connection to the Coulomb gas is established. In section 4, we calculate the expectation value of loops surrounding two points, which in the scaling limit, is in accordance with that of  $\text{CLE}_4$  and so with that of the level lines of the GFF at certain heights. We also compute the one-point function and comment on the calculation of some related observables. In section 5, we revisit the boundary monomer-dimer problem and calculate the partition function in the presence of two and four monomers, and a single monomer on the boundary. We can particularly check the latter to be in agreement with the result in [53]. In section 6, the left-passage probability is addressed and we find the approximation of the result for a very large lattice consistent with what is expected for the chordal  $\text{SLE}_4$  on a rectangular domain. Some less relevant, but still useful formulas have been moved to the appendix A. We also obtain a hitherto unknown series identity in the appendix B.

## 2 Grassmannian representation of the dimer model

For any dimer model on a finite graph, there is an adjacency matrix which has indices representing vertices of the graph, and entries equal the fugacities of bonds and zero otherwise. The partition function of the dimer model is then the hafnian of the adjacency matrix. However, even the permanent of a  $(0, 1)$ -matrix, which appears to be a less computationally complicated object than the hafnian, is not tractable in general [55]. A theorem due to Kasteleyn [41] guarantees that for any planar graph, there is an associated signed adjacency matrix, a Kasteleyn matrix, which the partition function of the dimer model is the Pfaffian (the square root of the determinant) of this matrix. The partition function of the double-dimer model is then the determinant of the relevant Kasteleyn matrix. Here we study the uniform double-dimer model (based on two uniform dimer model) on finite sublattices of the square grid, by a priori non-combinatorial approach through Grassmannian representation of the dimer model.

For pedagogical reasons, we first compute the partition function of the uniform dimer model (equiprobable dimer covers) when the square lattice is embedded on the cylinder, i.e. the boundary conditions are periodic and free along the horizontal and vertical directions respectively. For a lattice of size  $M \times N$ ,  $M$  and/or  $N$  even, it can be written as

$$\mathcal{Q}_0 = \int \prod_{n=1}^N \prod_{m=1}^M d\eta_{mn} (1 + \eta_{mn}\eta_{m+1n})(1 + \eta_{mn}\eta_{mn+1}) \quad (2)$$

with the periodic/free boundary conditions:  $\eta_{M+1n} = \eta_{1n}$ ,  $\eta_{mN+1} = 0$ , where  $\eta_{mn}$  are commuting nilpotent variables attached to every site, satisfying  $\eta_{mn}^2 = 0$ , to prevent double occupancy of a site by two dimers, and  $\int d\eta_{mn}\eta_{mn} = 1$  and  $\int d\eta_{mn} = 0$ , to ensure that each site is met by a dimer. The zero index of the partition function indicates the non-existence of defects (monomers) in the system, i.e. we deal with the pure close-packed dimer problem.

The representation (2) of the partition function is identical to the Hafnian of the adjacency matrix of the underlying square lattice. In accordance with Kasteleyn's theorem, we have to replace (2) with a representation identical to the Pfaffian of some related matrix. Following Hayn and Plechko [52] closely, we can introduce a set of completely anticommuting Grassmann variables  $\{a_{mn}, \bar{a}_{mn}\}$  and  $\{b_{mn}, \bar{b}_{mn}\}$  (so with the same calculus as  $\{\eta_{mn}\}$ ) for horizontal and vertical bonds respectively, such that

$$\begin{aligned} 1 + \eta_{mn}\eta_{m+1n} &= \int d\bar{a}_{mn} da_{mn} e^{a_{mn}\bar{a}_{mn}} (1 + a_{mn}\eta_{mn})(1 + \bar{a}_{mn}\eta_{m+1n}) \\ 1 + \eta_{mn}\eta_{mn+1} &= \int d\bar{b}_{mn} db_{mn} e^{b_{mn}\bar{b}_{mn}} (1 + b_{mn}\eta_{mn})(1 + \bar{b}_{mn}\eta_{mn+1}). \end{aligned} \quad (3)$$

We further introduce the notation  $\{A_{mn}, \bar{A}_{mn}, B_{mn}, \bar{B}_{mn}\}$ ,

$$\begin{aligned} A_{mn} &= 1 + a_{mn}\eta_{mn}, & \bar{A}_{m+1n} &= 1 + \bar{a}_{mn}\eta_{m+1n} \\ B_{mn} &= 1 + b_{mn}\eta_{mn}, & \bar{B}_{mn+1} &= 1 + \bar{b}_{mn}\eta_{mn+1} \end{aligned}$$

which are simply non-commuting Grassmann factors made use of for brevity. Thanks to the mirror-ordering method [56], the partition function can then be written as

$$\mathcal{Q}_0 = \text{Sp}_{\{a, \bar{a}, b, \bar{b}, \eta\}} \prod_{n=1}^N \left( \prod_{m=1}^M \overleftarrow{B}_{mn} \prod_{m=1}^M \overrightarrow{\bar{A}_{mn} \bar{B}_{mn} A_{mn}} \right), \quad (4)$$

where  $\text{Sp}_{\{\cdot\}}$  stands for the Gaussian averaging  $\int d\bar{a} da d\bar{b} db e^{a\bar{a} + b\bar{b}}(\dots)$ , as well as the integration over nilpotent variables  $\{\eta\}$ , and arrows indicate the direction of increasing in the index "m". This way, the individual  $\eta_{mn}$  can be isolated and integrated to yield a purely Grassmannian representation of the partition function of the dimer model:

$$\mathcal{Q}_0 = \text{Sp}_{\{a, \bar{a}, b, \bar{b}\}} \prod_{m,n} L_{mn}, \quad L_{mn} = a_{mn} + b_{mn} + \bar{a}_{m-1n} + (-1)^{m+1} \bar{b}_{mn-1}.$$

where the factor  $(-1)^{m+1}$  arises as the result of translating anticommuting variables  $L_{mn}$  through Grassmann factors  $\bar{B}_{mn}$ , from meeting point to the left. With the aid of additional Grassmann variables  $c_{mn}$  defined by the identity  $L_{mn} = \int dc_{mn} \exp(c_{mn} L_{mn})$ , the final expression is:

$$\mathcal{Q}_0 = \int \prod_{n=1}^N \prod_{m=1}^M \overrightarrow{dc_{mn}} \exp \left\{ \sum_{m=1}^M \sum_{n=1}^N [c_{m+1n} c_{mn} + (-1)^{m+1} c_{mn+1} c_{mn}] \right\} \quad (5)$$

Without loss of generality, we assume that  $\frac{M}{2}$  is an even integer. This imposes aperiodic boundary conditions for fermions (Grassmann variables) in horizontal direction,  $c_{M+1n} = -c_{1n}$ , because of the transposition of the products of the boundary Grassmann factors. Combinatorially, it is identical to compensating the minus sign due to the even cyclic permutation around the cylinder in the expansion of the determinant of Kasteleyn's matrix. As a result, we have to use half-integer momenta in Fourier substitution (in horizontal direction) for fermionic variables. Remember free boundary conditions in vertical direction,  $c_{mN+1} = 0$ , we can pass into momentum space through the transformation [52]

$$c_{mn} = \sqrt{\frac{2}{M(N+1)}} i^n \sum_{p=1}^M \sum_{q=1}^N c_{pq} e^{i \frac{\pi(2p-1)m}{M}} \sin \frac{\pi q n}{N+1} \quad (6)$$

Using the rules (60) and (61), the partition function (5) factorizes into the product of the determinants of similar matrices

$$\begin{bmatrix} 0 & 2i \cos \frac{\pi q}{N+1} & 0 & -2i \sin \frac{\pi(2p-1)}{M} \\ -2i \cos \frac{\pi q}{N+1} & 0 & -2i \sin \frac{\pi(2p-1)}{M} & 0 \\ 0 & 2i \sin \frac{\pi(2p-1)}{M} & 0 & 2i \cos \frac{\pi q}{N+1} \\ 2i \sin \frac{\pi(2p-1)}{M} & 0 & -2i \cos \frac{\pi q}{N+1} & 0 \end{bmatrix}$$

which, with a little abuse of notation  $-q \equiv N+1-q$ , indicating the coupling coefficients of the vector  $(c_{pq}, c_{\frac{M}{2}-pq}, c_{\frac{M}{2}-1+pq}, c_{M-pq})^t$  with the vector  $(c_{p-q}, c_{\frac{M}{2}-p-q}, c_{\frac{M}{2}-1+p-q}, c_{M-p-q})$ . For  $N$  even, these lead to the final evaluation of the partition function

$$\mathcal{Q}_0 = \prod_{p=1}^{\frac{M}{2}} \prod_{q=1}^{\frac{N}{2}} \left[ 4 \cos^2 \frac{\pi q}{N+1} + 4 \sin^2 \frac{\pi(2p-1)}{M} \right], \quad (N \text{ even}) \quad (7)$$

For  $N$  odd, the only difference is that there is a single uncoupled mode due to  $q = \frac{N+1}{2}$ , so the result is

$$\mathcal{Q}_0 = 2 \prod_{p=1}^{\frac{M}{2}} \prod_{q=1}^{\frac{N-1}{2}} \left[ 4 \cos^2 \frac{\pi q}{N+1} + 4 \sin^2 \frac{\pi(2p-1)}{M} \right], \quad (N \text{ odd}) \quad (8)$$

in agreement with the results in [41, 42].

The results (7) and (8) can also be obtained by a little different method. Indeed for our further analysis of the model, it is more convenient if we do Fourier transformation only for one of the indices and use combinatorics in compensation.

Back to the Grassmannian partition function (5), we do Fourier substitution in vertical direction, so (6) is replaced by

$$c_{mn} = \sqrt{\frac{2}{N+1}} i^n \sum_{q=1}^N c_{mq} \sin \frac{\pi q n}{N+1} \quad (9)$$

An overall minus sign or the factor  $i$ , that may occur in the calculation of partition functions in various situations, does not matter since they are always absorbed by the Jacobian determinant which is trivial here. So we are only concerned with the absolute value of the final results though we have to be careful about the signs of the terms with respect to each other. Here in this case the action becomes

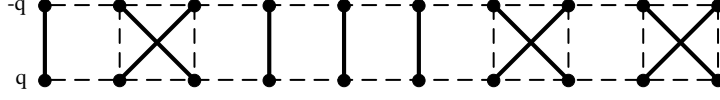


Figure 1: An instance of coupled Fourier modes  $q$  and  $-q$ , for a square lattice with  $M = 10$ . Each cross-form has weight one, and each vertical "dimer" has weight  $2 \cos \frac{\pi q}{N+1}$ .

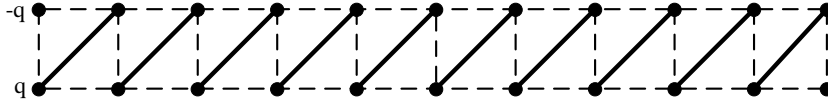


Figure 2: An additional admissible state thanks to the cylindrical boundary conditions. The first and last vertical lines are identified.

$$\mathcal{S}_0 = \sum_{q=1}^N \left\{ \sum_m \left[ -c_{m+1}c_{m-q} - i(-1)^{m+1} \cos \frac{\pi q}{N+1} c_{mq}c_{m-q} \right] \right\} \quad (10)$$

Equation (10) represents the conversion of the dimer model on the square lattice into some similar model on decoupled strips, each represents the coupling between two Fourier modes  $q$  and  $-q$ . These strips are no longer subgraphs of the square lattice and in fact, they are non-planar as an effect of Fourier transformation (figure 1). On a given strip, every vertical dimer (with a formal use of the word) has the fugacity, or rather weight, of  $2 \cos \frac{\pi q}{N+1}$  and the contribution of every cross-form is the factor 1. We need not worry about  $i$  and the minus signs at the moment, as they would always be absorbed to make every term in the expansion of the partition function have the same sign. For example, we can notice that on every strip, each vertical dimer and its closest next one have opposite parity in position. So, multiplying the coefficient of each vertical dimer with that of the next one yield to a plus sign. For  $M$  even, there is an integer number of these couples in every configuration on a strip, and each term is then positive.

In the absence of block diagonalization of the corresponding Kasteleyn's matrix, we use combinatorics to compute the number of dimer covers on a cylindrical strip. For  $N$  even, the partition function is

$$\mathcal{Q}_0 = \prod_{q=1}^{\frac{N}{2}} \left[ \left\{ \sum_{p=0}^{\frac{M}{2}} \left[ \binom{M-p}{p} + \binom{M-p-1}{p-1} \right] (2 \cos \frac{\pi q}{N+1})^{M-2p} \right\} + 2 \right], \quad (N \text{ even}) \quad (11)$$

included the two possibilities of a chain of tilted dimers due to the cylindrical boundary conditions in horizontal direction (figure 2). For  $N$  odd, the single mode  $q = \frac{N+1}{2}$  is represented by a one-dimensional dimer model on a line, which has a configuration space with only two members. The partition function becomes

$$\mathcal{Q}_0 = 2 \prod_{q=1}^{\frac{N-1}{2}} \left[ \left\{ \sum_{p=0}^{\frac{M}{2}} \left[ \binom{M-p}{p} + \binom{M-p-1}{p-1} \right] (2 \cos \frac{\pi q}{N+1})^{M-2p} \right\} + 2 \right], \quad (N \text{ odd}) \quad (12)$$

Similarly, we can calculate the partition function of the dimer model with the free boundary conditions,  $c_{M+1n} = 0$ ,  $c_{mN+1} = 0$ . It is

$$\mathcal{Q}_0 = \prod_{q=1}^{\frac{N}{2}} \left[ \sum_{p=0}^{\frac{M}{2}} \binom{M-p}{p} \left( 2 \cos \frac{\pi q}{N+1} \right)^{M-2p} \right] \quad (13)$$

for  $N$  even, and

$$\mathcal{Q}_0 = 2 \prod_{q=1}^{\frac{N-1}{2}} \left[ \sum_{p=0}^{\frac{M}{2}} \binom{M-p}{p} \left( 2 \cos \frac{\pi q}{N+1} \right)^{M-2p} \right] \quad (14)$$

for  $N$  odd.

We may note that (11)-(14) are associated with the Chebyshev polynomials of the second kind  $U_n(x) = \sin(n+1)\theta / \sin \theta$ ,  $\cos \theta = x$ , which can be shown by using the formula (62). We can also check that the partition functions (11)-(14) are identical to (7), (8) and (1), with the aid of the identities (64) and (65).

In the coming sections, we will use this approach to compute some observables defined on specific collections of double-dimer loops. These observables are supposed to make a strong connection between the scaling limit of the double-dimer model and the CLE with  $\kappa = 4$ .

### 3 Loops around the cylinder

We can find the distribution of the number of nontrivial loops in the uniform double-dimer model on the cylinder, through the previous semi-combinatorial approach. This case is specially simple because the Kasteleyn matrix can be diagonalized. We arrange some auxiliary fugacities  $\lambda$  and  $\lambda^{-1}$  in the two contributing dimer models, so that two conditions are satisfied; (1) each nontrivial loop (around the annulus) has to contribute exactly one  $\lambda$  or one  $\lambda^{-1}$ , and (2) trivial loops and loops with zero area

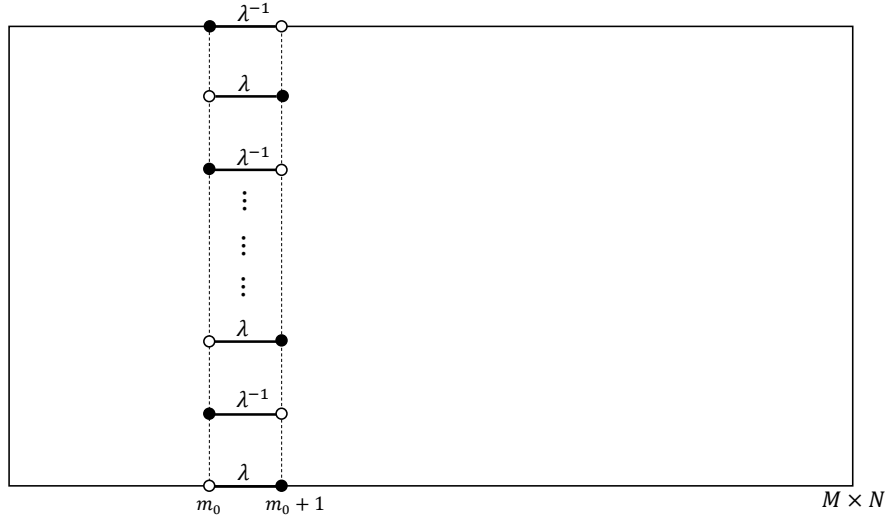


Figure 3: The arrangement of fugacities in one of the dimer models. Other bonds have fugacity 1.

(doubled edges) have to contribute the factor 1, in each term in the expansion of partition function of the double-dimer model. To this end, in one dimer model we insert the weights  $\lambda$  and  $\lambda^{-1}$ , for some column of bonds  $\{(m_0n, m_0 + 1n)\}$ , alternatively (figure 3). let's call such column the  $m_0$ -column. For our purpose,  $\lambda = e^{i\beta}$  is suitable. Of course it will not necessarily lead to a probability measure for the dimer model <sup>1</sup>, but it will be one for the double-dimer model if one dimer model has fugacities

<sup>1</sup>It is nevertheless a probability measure in the case of a cylindrical domain with even vertical length ( $N$  even) because of the balance between the number of dimers with  $\lambda$  and  $\lambda^{-1}$  fugacities in every dimer cover.

complex conjugate of those of the other, and if  $\beta$  is sufficiently small. We do so, and check if the above requirements are met. Each nontrivial loop crosses the  $m_0$ -column odd number of times, and each trivial loop even number of times. It is clear that the contribution of doubled edges is then the factor 1. So it is sufficient to show that the contribution of any loop crosses the  $m_0$ -column  $l$  times, in each term in the expansion of the partition function is  $\lambda^{\pm l(\text{mod } 2)}$ . It indeed holds because of the bipartiteness of the lattice, and the construction of the loops; each loop is a sequence of dimers, alternatively belong to one of the contributing dimer models. If, for example, we move on a loop from one cross of the  $m_0$ -column made by the loop to the other, we will pass the set of weight  $\{\lambda, \lambda^{-1}\}$  precisely. So the contribution of each loop only depends on the parity of the number of crosses of the  $m_0$ -column made by the loop. There is always two equiprobable possibilities of such contributions for each loop. The partition function is then the expectation of  $(\frac{e^{i\beta} + e^{-i\beta}}{2})^k$  or equally  $(\cos \beta)^k$ , where  $k$  indicates the number of loops around the annulus in each configuration of the double-dimer model on the cylinder. The reason for dividing by 2 is that the weight of any double-dimer configuration with  $n$  loops is proportional to  $2^n$ . If we orient the loops independently with equal probability, this expectation is somehow the discrete analog of the expectation of the layering operator,  $e^{i\beta N_l}$ , introduced in [34] for the Brownian Loop Soup (BLS) though the outcomes are very different in nature.

In conclusion, we have the following identity,

$$\begin{aligned} \langle (\cos \beta)^k \rangle_{dd} &= \mathcal{Z}_\beta / \mathcal{Z}_0 \\ &= \mathcal{Q}_\beta \mathcal{Q}_{-\beta} / \mathcal{Q}_0^2 \end{aligned} \quad (15)$$

where the index  $dd$  indicates that the expectation is with respect to the probability measure of the double-dimer model,  $\mathcal{Z}$  stands for the partition function of the resulting double-dimer model,  $\mathcal{Q}_\beta$  is the partition function of the dimer model with the above weights, and  $\mathcal{Q}_0$  is the partition function (11) or (12) depending on  $N$  being even or odd (In the case  $M$  odd and  $N$  even, there is simply no nontrivial loop). To compute the RHS of (15), we write the action for one contributing dimer model

$$\begin{aligned} \mathcal{S}_\beta &= \sum_{m \neq m_0} \sum_n \{c_{m+1n} c_{mn} + (-1)^{m+1} c_{mn+1} c_{mn}\} \\ &\quad + \sum_{n \text{ odd}} \lambda c_{m_0+1n} c_{m_0n} + \sum_{n \text{ even}} \lambda^{-1} c_{m_0+1n} c_{m_0n}, \quad \lambda = e^{i\beta} \end{aligned} \quad (16)$$

If the last two terms in (16) is written  $\sum_n (\cos \beta) c_{m_0+1n} c_{m_0n} + \sum_n (-1)^{n+1} (i \sin \beta) c_{m_0+1n} c_{m_0n}$ , after Fourier transformation (9) the action becomes

$$\begin{aligned} \mathcal{S}_\beta &= \sum_{q=1}^N \left\{ \sum_{m \neq m_0} \left[ -c_{m+1q} c_{m-q} - i(-1)^{m+1} \cos \frac{\pi q}{N+1} c_{mq} c_{m-q} \right] \right. \\ &\quad \left. - \cos \beta c_{m_0+1q} c_{m_0-q} - i \sin \beta c_{m_0+1q} c_{m_0q} \right\} \end{aligned} \quad (17)$$

Here the argument is as before with a little change in the fugacities and form of the strips after Fourier transformation. On any cylindrical strip  $[q, -q]$  there still exist cross-forms and vertical dimers, but just on the square  $\{(m_0, q), (m_0 + 1, q), (m_0 + 1, -q), (m_0, -q)\}$  (let's call it  $m_0$ -square) there is an additional possibility of two horizontal dimers, and they always come together to make an admissible configuration. For either a cross-form or two horizontal dimers on  $m_0$ -square, the overall final factor  $1 (= \cos^2 \beta + \sin^2 \beta)$  appears, the same as what occurs for a cross-form in the uniform case (figure 4). So the solution is also the same except that now the two situations when a chain of tilted dimers occur, add the weight of  $2 \cos \beta$  (instead of 2) to the solution for each strip. For  $N$  even, the result is

$$\mathcal{Q}_\beta = \prod_{q=1}^{\frac{N}{2}} \left[ \left\{ \sum_{p=0}^{\frac{M}{2}} \left[ \binom{M-p}{p} + \binom{M-p-1}{p-1} \right] \left( 2 \cos \frac{\pi q}{N+1} \right)^{M-2p} \right\} + 2 \cos \beta \right], \quad (N \text{ even}) \quad (18)$$



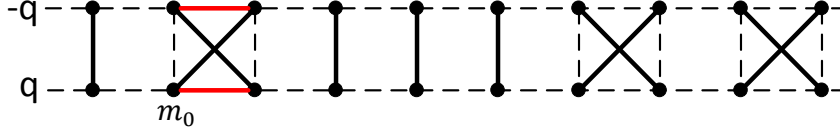


Figure 4: An instance of coupled Fourier modes  $q$  and  $-q$  for the situation in figure 3. The pair of red horizontal "dimers" is possible only in the  $m_0$ -column.

By using the identity (65) we can show that  $\mathcal{Z}_\beta = \mathcal{Q}_\beta \mathcal{Q}_{-\beta}$  is the determinant of the associated Kasteleyn matrix [38].

For  $N$  odd,  $\mathcal{Q}_\beta$  does not yield a probability measure because of the single mode  $q = \frac{N+1}{2}$  which produces the factor  $(1 + e^{i\beta})$  in the partition function of the dimer model,

$$\mathcal{Q}_\beta = (1 + e^{i\beta}) \prod_{q=1}^{\frac{N-1}{2}} \left[ \left\{ \sum_{p=0}^{\frac{M}{2}} \left[ \binom{M-p}{p} + \binom{M-p-1}{p-1} \right] (2 \cos \frac{\pi q}{N+1})^{M-2p} \right\} + 2 \cos \beta \right], \quad (N \text{ odd}) \quad (19)$$

The resulting double-dimer partition function is nevertheless real. For a very large lattice, things go on as in [38], but we believe the result is

$$\sum_{k=0}^{\infty} \mathbb{P}(k \text{ loops}) (\cos \beta)^k = \prod_{\substack{j=1 \\ j \text{ odd}}}^{\infty} \frac{(1 + 2\eta^j \cos \beta + \eta^{2j})^2}{(1 + \eta^j)^4} \quad (20)$$

for  $N$  even, and

$$\sum_{k=0}^{\infty} \mathbb{P}(k \text{ loops}) (\cos \beta)^k = \frac{1 + \cos \beta}{2} \prod_{\substack{j=2 \\ j \text{ even}}}^{\infty} \frac{(1 + 2\eta^j \cos \beta + \eta^{2j})^2}{(1 + \eta^j)^4} \quad (21)$$

for  $N$  odd, where  $\eta = e^{-\frac{M}{2N}\pi}$ . On the other hand, if further  $M \ll N$ , we can somehow approximate the expectation (15)

$$\ln(\langle (\cos \beta)^k \rangle) \approx \frac{2N}{\pi} \int \ln(1 - \frac{2b f(x)}{(1 + f(x))^2}) \frac{1}{\sqrt{1-x^2}} dx \quad (22)$$

where  $b = 1 - \cos \beta$ ,  $x = \cos \frac{\pi q}{N+1}$ , and  $f(x) = (\sqrt{x^2 + 1} - x)^M$ . Because of the intense concentration of the integrand near  $x = 0$ , we can neglect  $\frac{1}{\sqrt{1-x^2}}$  and replace  $f(x)$  by  $\frac{-f'(x)}{M}$ . With differentiating (22) with respect to  $b$  (for the moment in range where there is no singularity) and changing the order of integration, we obtain

$$\sum_{k=0}^{\infty} \mathbb{P}(k \text{ loops}) (\cos \beta)^k \approx \exp \left( -\frac{N}{M} \frac{\beta^2}{\pi} \right) \quad (23)$$

To make an explicit connection with Coulomb gas formalism as well as check (23), we calculate a related observable which is very similar in quantity. Suppose in each dimer model above (but now  $M$  and  $N$  are odd), we insert a single monomer on the corner (see section 5), one at the top-left side and one at the down-left side, and further do likewise. There is always a path of dimers in the arising double-dimer model, which connects the top boundary of the cylinder to the bottom. In this case, the

partition function of the double-dimer model leads to the distribution of the winding number of the path around the cylinder, that is

$$\begin{aligned} \sum_{k=0}^{\infty} \mathbb{P}(k \text{ windings}) (\cos \beta)^k &= \mathcal{Z}_{\beta} \\ &= \prod_{\substack{q=1 \\ q \neq \frac{N+1}{2}}}^N \left[ \left\{ \sum_{p=0}^{\frac{M}{2}} \left[ \binom{M-p}{p} + \binom{M-p-1}{p-1} \right] (2 \cos \frac{\pi q}{N+1})^{M-2p} \right\} + 2 \cos \beta \right] \end{aligned} \quad (24)$$

Motivated by [34], we call the LHS of (24) the expectation of the winding operator,  $e^{i\beta N_w}$ , where the orientation of each winding is considered with equal probability. For a very large lattice, we have

$$\sum_{k=0}^{\infty} \mathbb{P}(k \text{ windings}) (\cos \beta)^k = \prod_{\substack{j=2 \\ j \text{ even}}}^{\infty} \frac{(1 + 2\eta^j \cos \beta + \eta^{2j})^2}{(1 + \eta^j)^4} \quad (25)$$

which for  $M \ll N$  becomes

$$\sum_{k=0}^{\infty} \mathbb{P}(k \text{ windings}) (\cos \beta)^k \approx \frac{2}{1 + \cos \beta} \exp \left( -\frac{N}{M} \frac{\beta^2}{\pi} \right) \quad (26)$$

If we interpret (26) in terms of height fluctuations in the dual picture [39], the LHS is the correlator of the exponential of the height, where the heights are taken to be integer multiples of  $\pi$ . The result is consistent with that of the Coulomb gas method for the simple Gaussian model on a very long cylinder [19].

## 4 Loops surrounding two points

We can use the the previous method to formally write the distribution of the number of loops surrounding an arbitrary number of faces (vertices of the dual) of the square lattice  $M \times N$ . For two faces for example, assuming their centers to be located at  $(M_1 + \frac{1}{2}, N_1 + \frac{1}{2})$  and  $(M_2 + \frac{1}{2}, N_2 + \frac{1}{2})$ , for one dimer model we insert the weights  $\lambda_1$  and  $\lambda_1^{-1}$ , alternatively on the column of bonds  $\{(M_1 n, M_1 + 1n)\}, n \leq N_1$ , and likewise for another column replacing the index "1" by "2". We consider the conjugate of these weights for the other dimer model, and further assume that  $M_1$  and  $M_2$ , as well as  $N_1$  and  $N_2$  have the same parity. Based on the arguments in the previous sections, one can show that in the expansion of the partition function of the double-dimer model, the coefficient of  $(\cos(\beta_1 + \beta_2))^k (\cos \beta_1)^{k_1} (\cos \beta_2)^{k_2}$  is proportional to the probability of occurring  $k$  loops surrounding both points "1" and "2",  $k_1$  loops around the point "1" but not "2", and  $k_2$  loops around the point "2" but not "1". In this case however, the complexity of the situation grows too fast with the exponents of  $\lambda_1$  and  $\lambda_2$  that a combinatorial analysis of the whole problem fails. In fact, even the previous decoupling to strips can not be met because of the lack of enough homogeneity in the model. Still, we can manage to compute the expectation of the number of loops surrounding the points. Let's slightly modify the weights above and replace  $\lambda_1$  (respectively  $\lambda_1^{-1}$ ) with  $1 + \epsilon_1$  (respectively  $1 - \epsilon_1$ ), and do likewise for the index "2" (figure 5). If  $\mathcal{Q}_{\epsilon_1, \epsilon_2}$  is the partition function of the associated dimer model and  $\mathcal{Z}_{\epsilon_1, \epsilon_2}$  the corresponding one for the double-dimer model coming out of the identity  $\mathcal{Z}_{\epsilon_1, \epsilon_2} = \mathcal{Q}_{\epsilon_1, \epsilon_2} \mathcal{Q}_{-\epsilon_1, -\epsilon_2}$ , the coefficient of  $\epsilon_1 \epsilon_2$  in the expansion of  $\mathcal{Z}_{\epsilon_1, \epsilon_2}$  is then proportional to  $\langle N_{12} \rangle$ , the expectation of the number of loops surrounding both points "1" and "2", precisely

$$\langle N_{12} \rangle = \frac{2C_{12}}{\mathcal{Q}_0} - \frac{2C_1 C_2}{\mathcal{Q}_0^2} \quad (27)$$

where  $C_1$ ,  $C_2$  and  $C_{12}$  are determined by the following expansion

$$\mathcal{Q}_{\epsilon_1, \epsilon_2} = \mathcal{Q}_0 + C_1 \epsilon_1 + C_2 \epsilon_2 + C_{12} \epsilon_1 \epsilon_2 + O(\epsilon_1^2) + O(\epsilon_2^2) \quad (28)$$

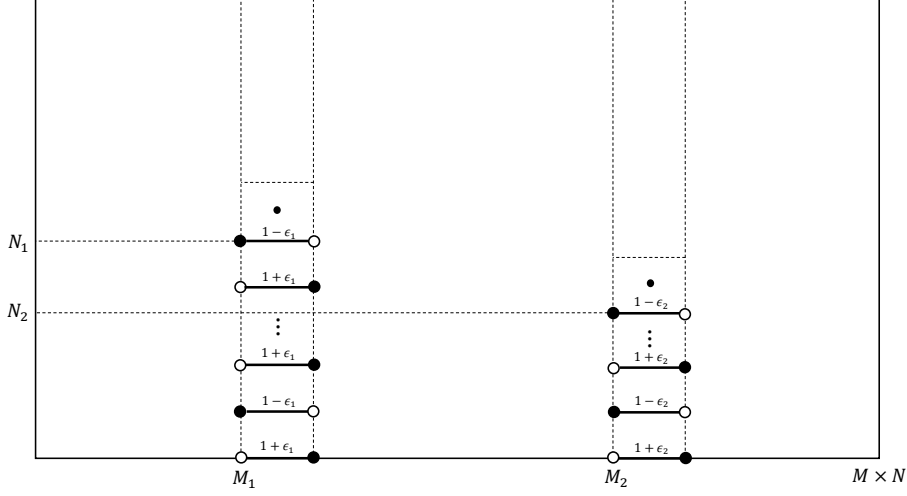


Figure 5: The arrangement of fugacities in  $M_1$ - and  $M_2$ -columns, in one of the dimer models.

To compute these coefficients, we again do Fourier transformation (9) for the Grassmannian action of the partition function  $\mathcal{Q}_{\epsilon_1, \epsilon_2}$  with the free boundary conditions for Grassmann variables,  $c_{M+1n} = c_{mN+1} = 0$ . The action becomes

$$\begin{aligned} \mathcal{S}_{\epsilon_1, \epsilon_2} = & \sum_{m=1}^M \sum_{q=1}^N \left\{ -c_{m+1q} c_{m-q} - i(-1)^{m+1} \cos \frac{\pi q}{N+1} c_{mq} c_{m-q} \right\} \\ & - \epsilon_1 \sum_{n_1=1}^{N_1} \frac{2}{N+1} \sum_{q, q'=1}^N c_{M_1+1q} c_{M_1 q'} \sin \frac{\pi q n_1}{N+1} \sin \frac{\pi q' n_1}{N+1} \\ & - \epsilon_2 \sum_{n_2=1}^{N_1} \frac{2}{N+1} \sum_{q, q'=1}^N c_{M_2+1q} c_{M_2 q'} \sin \frac{\pi q n_2}{N+1} \sin \frac{\pi q' n_2}{N+1} \end{aligned} \quad (29)$$

The first row in (29) gives  $\mathcal{Q}_0$  in terms of the multiplication of the contributions of coupled Fourier modes  $q$  and  $-q \equiv N+1-q$ , that is (13). We replace  $\mathcal{Q}_0$  in (13) by  $\mathcal{Q}'_{q_0}$  and  $\mathcal{Q}''_{q_1, q_2}$  when we exclude the contribution of the mode  $q_0$  and modes  $q_1$  and  $q_2$ , respectively from the multiplication. For the coefficient  $C_i$ , one of the terms in the second or the third row in (29) contributes in configurations, that is, the weight of one of the bonds in the cross-form sitting in the  $M_i$ -square is changed to  $\epsilon_i$ . However, the style of couplings between Fourier modes will not change and the structure remains the same as before. The result is

$$C_i = \sum_{n_i=1}^{N_i} \sum_{q_0=1}^{\frac{N}{2}} A_{q_0}^{(n_i)} \mathcal{Q}'_{q_0}, \quad i = 1, 2 \quad (30)$$

where by  $A_{q_0}^{(n_i)}$  we mean

$$A_{q_0}^{(n_i)} = \frac{4}{N+1} (-1)^{n_i+1} \sin^2 \frac{\pi q_0 n_i}{N+1} \Theta_{i, q_0} \quad (31)$$

where  $\Theta_{i, q_0} = \sum_{p=0}^{\frac{M-2}{2}} \left[ \sum_{k=0}^p \binom{M_i - 1 - k}{k} \binom{M - M_i - 1 - (p - k)}{p - k} \right] (2 \cos \frac{\pi q_0}{N+1})^{M-2-2p}.$

But the situation for the coefficient of  $\epsilon_1 \epsilon_2$  is more complicated; there can be terms supporting two "unusual" bonds between two different strips  $[q_1, -q_1]$  and  $[q_2, -q_2]$ , and we have to be careful about the signs. Regarding this, the sign of a term, due to the contribution of two rows of the columns

$\{(M_1n, M_1 + 1n)\}$  and  $\{(M_2n, M_2 + 1n)\}$ , naturally depends only on the parity of vertical indices of the rows with respect to each other. For an "unusual" state, either it also depends on the parity of horizontal indices of the columns with respect to each other (figure 6), or it is independent of any index (figure 7). The result can be expanded in three distinct kinds of terms

$$C_{12} = \sum_{n_1=1}^{N_1} \sum_{n_2=1}^{N_2} \left\{ \sum_{q_0=1}^{\frac{N}{2}} A_{q_0}^{(n_1, n_2)} \mathcal{Q}'_{q_0} + \sum_{q_1 \neq q_2} (A_{q_1, q_2}^{(n_1, n_2)} + B_{q_1, q_2}^{(n_1, n_2)}) \mathcal{Q}''_{q_1, q_2} \right\} \quad (32)$$

Along with some extra symbols,  $A_{q_0}^{(n_1, n_2)}$ ,  $A_{q_1, q_2}^{(n_1, n_2)}$  and  $B_{q_1, q_2}^{(n_1, n_2)}$  are

$$A_{q_0}^{(n_1, n_2)} = \left(\frac{4}{N+1}\right)^2 (-1)^{n_1+n_2} \sin^2 \frac{\pi q_0 n_1}{N+1} \sin^2 \frac{\pi q_0 n_2}{N+1} \Psi_{q_0},$$

$$A_{q_1, q_2}^{(n_1, n_2)} = \left(\frac{4}{N+1}\right)^2 (-1)^{n_1+n_2} \sin^2 \frac{\pi q_1 n_1}{N+1} \sin^2 \frac{\pi q_2 n_2}{N+1} \Xi_{q_1, q_2},$$

$$B_{q_1, q_2}^{(n_1, n_2)} = \left(\frac{2}{N+1}\right)^2 \sin \frac{\pi q_1 n_1}{N+1} \sin \frac{\pi q_2 n_1}{N+1} \sin \frac{\pi q_1 n_2}{N+1} \sin \frac{\pi q_2 n_2}{N+1} \left\{ (-1)^{M_2-M_1} (-1)^{n_1+n_2} \sum_{\delta, \delta'} \Delta_{q_1, q_2}^{\delta, \delta'} \right. \\ \left. + \sum_{\delta=\delta'} \Delta_{q_1, q_2}^{\delta, \delta'} - \sum_{\delta \neq \delta'} \Delta_{q_1, q_2}^{\delta, \delta'} \right\}.$$

where  $\delta$  and  $\delta'$  can only take two values 0 and 1. Here  $\Psi_{q_0}$ ,  $\Xi_{q_1, q_2}$  and  $\Delta_{q_1, q_2}^{\delta, \delta'}$  sum up the terms where both bonds with weights  $\epsilon_1$  and  $\epsilon_2$  are in the same strip, in two different strips, and connecting two different strips, respectively.

$$\Psi_{q_0} = \sum_{p=0}^{\frac{M-4}{2}} \left[ \sum_{p_1+p_2+p_3=p} \binom{M_1-1-p_1}{p_1} \binom{M_2-M_1-2-p_2}{p_2} \binom{M-M_2-1-p_3}{p_3} \right] \\ (2 \cos \frac{\pi q_0}{N+1})^{M-4-2p},$$

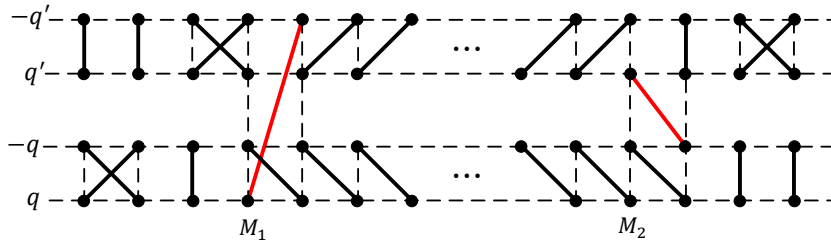


Figure 6: An example of an "unusual" state, whose sign depends on both horizontal and vertical indices.

$$\Xi_{q_1, q_2} = \left\{ \sum_{p_1=0}^{\frac{M-2}{2}} \left[ \sum_{k_1=0}^{p_1} \binom{M_1-1-k_1}{k_1} \binom{M-M_1-1-(p_1-k_1)}{p_1-k_1} \right] (2 \cos \frac{\pi q_1}{N+1})^{M-2-2p_1} \right\} \\ \left\{ \sum_{p_2=0}^{\frac{M-2}{2}} \left[ \sum_{k_2=0}^{p_2} \binom{M_2-1-k_2}{k_2} \binom{M-M_2-1-(p_2-k_2)}{p_2-k_2} \right] (2 \cos \frac{\pi q_2}{N+1})^{M-2-2p_2} \right\},$$

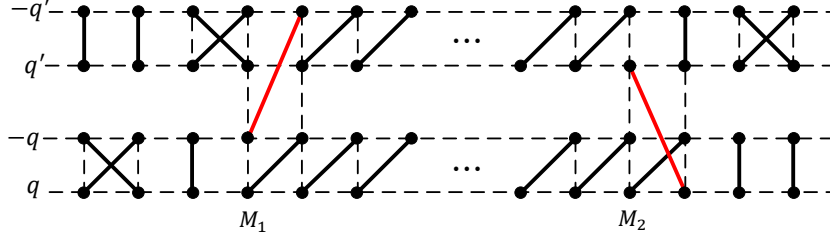


Figure 7: An example of an "unusual" state, whose sign is independent of any index.

$$\Delta_{q_1, q_2}^{\delta, \delta'} = \left\{ \sum_{p_1=0}^{\frac{M-(M_2-M_1)-2+\delta+\delta'}{2}} \left[ \sum_{k_1=0}^{p_1} \binom{M_1-1-k_1+\delta}{k_1} \binom{M-M_2-1-(p_1-k_1)+\delta'}{p_1-k_1} \right] \right. \\ \left. (2 \cos \frac{\pi q_1}{N+1})^{M-(M_2-M_1)-2-2p_1+\delta+\delta'} \right\} \\ \left\{ \sum_{p_2=0}^{\frac{M-(M_2-M_1)-\delta-\delta'}{2}} \left[ \sum_{k_2=0}^{p_2} \binom{M_1-k_2-\delta}{k_2} \binom{M-M_2-(p_2-k_2)-\delta'}{p_2-k_2} \right] \right. \\ \left. (2 \cos \frac{\pi q_2}{N+1})^{M-(M_2-M_1)-2p_2-\delta-\delta'} \right\}. \quad (33)$$

Remembering the relation between the partition function of the dimer model and Chebyshev polynomials,  $\mathcal{Q}_0 = \prod_{q=1}^{\frac{N}{2}} U_M(i \cos \frac{\pi q}{N+1})$ , the final result for  $\langle N_{12} \rangle$  is briefly

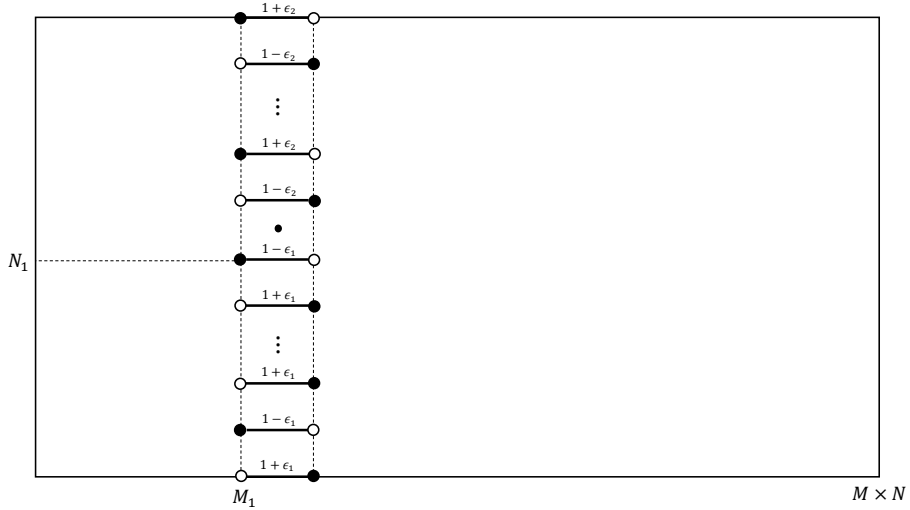


Figure 8: The arrangement of fugacities in  $M_1$ -column, in one of the dimer models.

$$\langle N_{12} \rangle = \sum_{n_1=1}^{N_1} \sum_{n_2=1}^{N_2} \left\{ 2 \sum_{q_0=1}^{\frac{N}{2}} \left( \frac{A_{q_0}^{(n_1, n_2)}}{U_M(q_0)} - \frac{A_{q_0}^{(n_1)} A_{q_0}^{(n_2)}}{U_M(q_0)^2} \right) + 2 \sum_{q_1 \neq q_2} \frac{B_{q_1, q_2}^{(n_1, n_2)}}{U_M(q_1) U_M(q_2)} \right\} \quad (34)$$

along with a little abuse of notation  $U_M(q) \equiv U_M(i \cos \frac{\pi q}{N+1})$ , where  $U_M(x)$  is the M-th Chebyshev polynomial of the second kind.

Another interesting situation, motivated by [34], is the so-called charge conservation condition, where we are interested in  $\langle N_{12'} + N_{1'2} \rangle$ , the expectation of the number of loops surrounding one face not the other, and vice versa. To make the situation clear, we first obtain  $\langle N_i^\odot \rangle$ , the expectation of the number of loops around one face. If we consider the above arrangement of fugacities (in both dimer models) only for one of the faces, say  $(M_1 + \frac{1}{2}, N_1 + \frac{1}{2})$ , a zero coefficient in the first order of  $\epsilon_1$  emerges in the expansion of the partition function of the double-dimer model. To avoid this, we insert fugacities  $1 \mp \epsilon_2$  on the bonds remained in the same column in one dimer model, and likewise in the other replacing  $\epsilon_2$  by  $-\epsilon_2$  (figure 8). For our purposes, the same is obtained if instead, we replace  $\epsilon_1$  by  $\epsilon_1 + \epsilon_2$  and look at the coefficient of  $\epsilon_1 \epsilon_2$  in the expansion. The desired expectation is

$$\langle N_1^\odot \rangle = 2 \left( \frac{C_1}{Q_0} \right)^2 \quad (35)$$

in terms of the above notations.

Suppose now we insert the above-mentioned column of fugacities also for the other face, but replace  $\epsilon_i$  by  $-\epsilon_i$  (figure 9). This arrangement of fugacities, again for our purposes, is identical to replacing  $\epsilon_1$  by  $\epsilon_1 + \epsilon_2$ , and  $-\epsilon_1$  by  $-(\epsilon_1 + \epsilon_2)$ . The coefficient of  $\epsilon_1 \epsilon_2$  is the expectation  $\langle N_{12'} + N_{1'2} \rangle$ , which is

$$\langle N_{12'} + N_{1'2} \rangle = 2 \left( \frac{C_1 + C_2}{Q_0} \right)^2 - 4 \frac{C_{12}}{Q_0} \quad (36)$$

We can see that the results (27), (35) and (36) are simultaneously consistent with each other.

With careful arranging of fugacities, many other observables such as generalizations of the above quantities to an arbitrary number of faces, the probability of some given dimers belonging to the same loop, n-point functions of dimer correlations in the dimer model, etc. can be computed similarly. For instance, the probability of two dimers,  $\{M_1 N_1, M_1 + 1 N_1\}$  and  $\{M_2 N_2, M_2 + 1 N_2\}$ , belonging to the same loop can be obtained by inserting the fugacities  $1 + \epsilon_1$  and  $1 + \epsilon_2$  on the corresponding bonds respectively, in one dimer model, and likewise replacing  $\epsilon_i$  by  $-\epsilon_i$  in the other. The desired probability is obtained from (34) by considering only the " $n_1 = N_1, n_2 = N_2$ " term in the summation " $\sum_{n_1} \sum_{n_2}$ ". This result would be expected since the expectation  $\langle N_{12} \rangle$  is the summation of all such probabilities

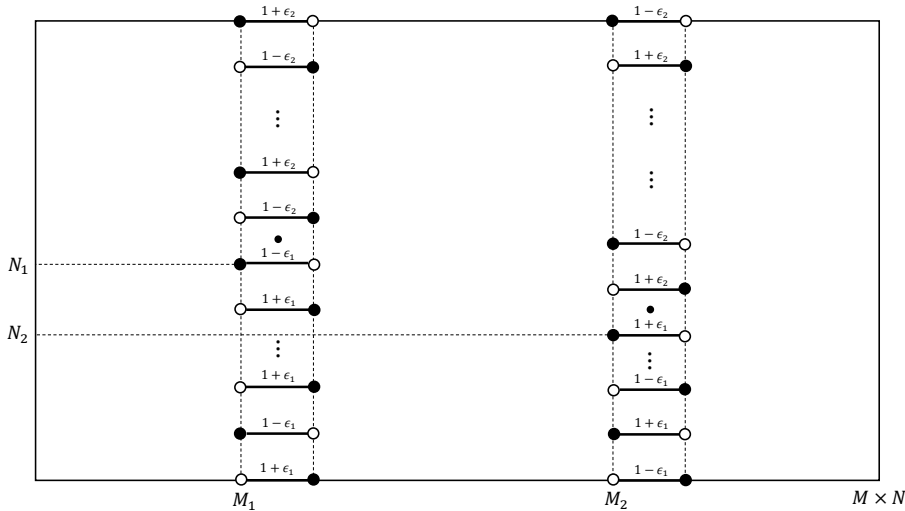


Figure 9: The arrangement of fugacities in  $M_1$ - and  $M_2$ -column, in one of the dimer models.

for relevant dimers.

After all, we are interested in the scaling limits of such observables <sup>2</sup>. Here we try to approximate (34) for very large lattices while keeping  $\frac{N}{M}$ ,  $\frac{N_1}{N}$ ,  $\frac{N_2}{N}$ ,  $\frac{M_1}{M}$  and  $\frac{M_2}{M}$  fixed. This case is especially interesting. First, we rewrite the expressions in (33), again using Chebyshev polynomials, for convenience and more insight into the result

$$\begin{aligned}\Theta_{i,q_0} &= U_{M_i-1}(q_0)U_{M-M_i-1}(q_0), \\ \Psi_{q_0} &= U_{M_1-1}(q_0)U_{M_2-M_1-2}(q_0)U_{M-M_2-1}(q_0), \\ \Delta_{q_1,q_2}^{\delta,\delta'} &= U_{M_1-1+\delta}(q_1)U_{M-M_2-1+\delta'}(q_1)U_{M_1-\delta}(q_2)U_{M-M_2-\delta'}(q_2)\end{aligned}\quad (37)$$

Now we note that each term in (34) is only significant when  $\cos \frac{\pi q_i}{N+1} \approx 0$ . On the other hand, for small  $\epsilon > 0$  and  $\theta = \frac{\pi}{2} + \epsilon$ ,  $\ln(x + \sqrt{1+x^2}) = \sinh^{-1} x$  leads to  $\sqrt{1 + \cos^2 \theta} + \cos \theta = \exp(\epsilon + O(\epsilon^3))$ . Regarding this and the identity  $U_n(q) = (2\sqrt{1 + \cos^2 \theta})^{-1}[(\sqrt{1 + \cos^2 \theta} + \cos \theta)^{n+1} - (-\sqrt{1 + \cos^2 \theta} + \cos \theta)^{n+1}]$ ,  $\theta = \frac{\pi q}{N+1}$ , for large  $n$  we conclude that <sup>3</sup>

$$U_n(q) \approx \begin{cases} \sinh(n\epsilon) & n \text{ odd} \\ \cosh(n\epsilon) & n \text{ even} \end{cases} \quad (38)$$

Without loss of generality, we assume that  $M_1$  and  $M_2 > M_1$  are both even, so for example  $U_M(q) \approx \cosh M\epsilon$ ,  $U_{M_2-M_1-2}(q) \approx \cosh(M_2 - M_1)\epsilon$ ,  $U_{M-M_1-1}(q) \approx \sinh(M - M_1)\epsilon$  and so on. These approximations will be exact in the thermodynamic limit. There are also some coefficients in front of  $\Theta_{q_0}$ ,  $\Psi_{q_0}$  and  $\Delta_{q_1,q_2}^{\delta,\delta'}$  in the expansion of (34) which are translated into suitable expressions. Finally, with the aid of the identities (66) and (67), and using  $\sum_\epsilon$  formally at the moment, we sum over  $n_1$  and  $n_2$  to obtain <sup>4</sup>

$$\begin{aligned}\langle N_{12} \rangle &\approx \frac{1}{2N^2} \sum_{\epsilon_0} \left\{ \frac{\sin(2N_1)\epsilon_0 \sin(2N_2)\epsilon_0}{\sin^2 \epsilon_0} \frac{\cosh(M - M_2 + M_1)(2\epsilon_0) - \cosh(M - M_2 - M_1)(2\epsilon_0)}{\cosh(2M\epsilon_0) + 1} \right\} \\ &+ \frac{1}{2N^2} \sum_{\epsilon_1 \neq \epsilon_2} \left\{ \frac{\sin(2N_1)\frac{\epsilon_1+\epsilon_2}{2} \sin(2N_2)\frac{\epsilon_1+\epsilon_2}{2}}{\sin^2 \frac{\epsilon_1+\epsilon_2}{2}} \frac{\cosh(M - M_2 + M_1)(\epsilon_1 + \epsilon_2) - \cosh(M - M_2 - M_1)(\epsilon_1 + \epsilon_2)}{\cosh M(\epsilon_1 + \epsilon_2) + \cosh M(\epsilon_1 - \epsilon_2)} \right. \\ &\left. + \frac{\sin(2N_1)\frac{\epsilon_1-\epsilon_2}{2} \sin(2N_2)\frac{\epsilon_1-\epsilon_2}{2}}{\sin^2 \frac{\epsilon_1-\epsilon_2}{2}} \frac{\cosh(M - M_2 + M_1)(\epsilon_1 - \epsilon_2) - \cosh(M - M_2 - M_1)(\epsilon_1 - \epsilon_2)}{\cosh M(\epsilon_1 + \epsilon_2) + \cosh M(\epsilon_1 - \epsilon_2)} \right\}\end{aligned}\quad (39)$$

where we choose the index "i" of the associated  $\epsilon$  according to the mode  $q_i$ . Many terms have disappeared in appreciation of larger and larger lattices.

Now we come to the point of identifying  $\epsilon_i$ 's. Take  $q = \frac{N}{2} + k$  then  $\epsilon = \frac{\pi(2k-1)}{2(N+1)}$ . So  $\epsilon_1 + \epsilon_2 = \frac{\pi(k_1+k_2-1)}{(N+1)}$  and  $\epsilon_1 - \epsilon_2 = \frac{\pi(k_1-k_2)}{(N+1)}$ . If we change the role of  $\epsilon_1 + \epsilon_2$  and  $\epsilon_1 - \epsilon_2$  in the second term of the second summation, (39) becomes

$$\begin{aligned}\langle N_{12} \rangle &\approx \sum_{j=1}^{\infty} \left\{ \frac{2}{\pi^2 j^2} \sin\left(\frac{N_1}{N}\pi j\right) \sin\left(\frac{N_2}{N}\pi j\right) \left[ \cosh\left(\frac{M - M_2 + M_1}{N}\pi j\right) - \cosh\left(\frac{M - M_2 - M_1}{N}\pi j\right) \right] \right. \\ &\quad \left. \sum_{k=-\infty}^{\infty} \frac{1}{\cosh\left(\frac{M}{N}\pi j\right) + \cosh\left(\frac{M}{N}\pi k\right)} \delta_{j+k-\frac{1}{2},0} \right\}\end{aligned}\quad (40)$$

<sup>2</sup>Though there is delicacy in the choice of the boundary conditions [38] and we have to be careful in taking the continuum limit, here we will not concern ourselves with the issue.

<sup>3</sup> Indeed this approximation has been used to obtain (20) and (21) in the previous section, as done in [38].

<sup>4</sup>Many necessary parentheses are ignored to make the appearance of the expressions more pleasant. We hope there will be no ambiguity about this.

where we use the approximation  $\sin \epsilon \approx \epsilon$  for small  $\epsilon$ . From (72) and (68), we conclude that in the thermodynamic limit

$$\langle N_{12} \rangle = \frac{8}{\pi^3} \frac{M}{N} \sum_{m,n=1}^{\infty} \frac{\sin(\frac{M_1}{M} m \pi) \sin(\frac{N_1}{N} n \pi) \sin(\frac{M_2}{M} m \pi) \sin(\frac{N_2}{N} n \pi)}{m^2 + (\frac{M}{N})^2 n^2} \quad (41)$$

This is proportional to the Green's function for the Dirichlet problem posed for the Laplace equation on any rectangle  $\{0 < x < a, 0 < y < b; \frac{a}{b} = \frac{M}{N}\}$  [57]. The result (41) seems to be consistent with that of CLE<sub>4</sub>.

## 5 Revisiting boundary monomer-dimer problem

We somewhat digress here and make use of the previous approach to simply solve the monomer-dimer problem where it is exactly solvable; the case of single monomer on the corner is relevant to the next section.

The inclusion of monomers is a priori equivalent to the insertion of magnetic fields at the locations of defect [53]. While this interpretation provides us with a noticeable physical insight into the monomer-dimer situation, as dislocality does not emerge in the boundary case (or some particular situations, see below.), there's no need to apply auxiliary variables representing magnetic fields, in our half-combinatorial approach; we directly compute the expectation of monomers in the action of the pure case.

Assume for example that there are two monomers on the boundary, on the same line at positions  $(m_1, 1)$  and  $(m_2, 1)$ ,  $m_1$  odd and  $m_2$  even, and  $m_1 < m_2$ . Each permissible configuration has two of the Fourier transformed variables sticking to some strip  $[q, -q]$  (figure 10), i.e. an extra multiplicative term of kind  $c_{m_1 q} c_{m_2 -q}$ ,  $q = 1, \dots, N$ , appears in front of every (valid) term in the expansion of the partition function of close-packed dimer case. The solution is:

$$\mathcal{Q}_{m_1, m_2} = \sum_{q_0=1}^{\frac{N}{2}} A_{q_0}^{\parallel} \mathcal{Q}'_{q_0} \quad (42)$$

where by  $A_{q_0}^{\parallel}$  we mean

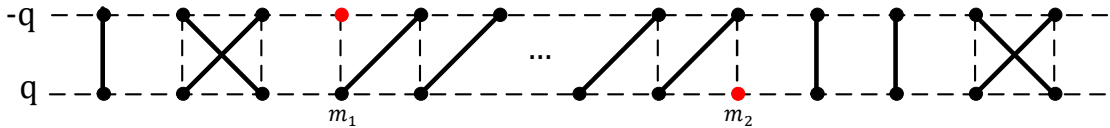


Figure 10: An instance of coupled Fourier modes  $q$  and  $-q$  in the presence of two monomers (in red) on the boundary.

$$A_{q_0}^{\parallel} = \frac{2(1 - (-1)^{m_2 - m_1})}{N+1} \sin^2 \frac{\pi q_0}{N+1} \sum_{p=0}^{\frac{M - (m_2 - m_1) - 1}{2}} \left[ \sum_{k=0}^p \binom{m_1 - 1 - k}{k} \binom{M - m_2 - (p - k)}{p - k} \right] (2 \cos \frac{\pi q_0}{N+1})^{M - (m_2 - m_1) - 1 - 2p} \quad (43)$$

The same is obtained if monomers are at positions  $(m_1, 1)$  and  $(m_2, N)$ ; it does not matter whether the monomers are on the same side or on the opposite sides <sup>5</sup>.

<sup>5</sup>In this case however, the monomers may have the same horizontal index.



For two monomers on the boundary, not inline and at positions  $(m_0, 1)$  and  $(M, n_0)$ , the partition function is:

$$\mathcal{Q}_{m_0, n_0} = \sum_{q_0=1}^{\frac{N}{2}} A_{q_0}^{\perp} \mathcal{Q}'_{q_0} \quad (44)$$

where  $A_{q_0}^{\perp}$  is:

$$A_{q_0}^{\perp} = \frac{2(1 - (-1)^{m_0})}{N+1} \sin \frac{\pi q_0}{N+1} \sin \frac{\pi q_0 n_0}{N+1} \left[ \sum_{p=0}^{\frac{m_0-1}{2}} \binom{m_0-1-p}{p} \left( 2 \cos \frac{\pi q_0}{N+1} \right)^{m_0-1-2p} \right] \quad (45)$$

It is straightforward to compute the partition function of the dimer model in the presence of  $2n$  number of monomers on the boundary. For example, if there are four inline monomers at  $(m_i, 1)$ ,  $i = 1, \dots, 4$  and  $m_i < m_j$  for  $i < j$ , then:

$$\mathcal{Q}_{m_1, m_2, m_3, m_4} = \sum_{q_0} A_{q_0}^{\parallel\parallel\parallel} \mathcal{Q}'_{q_0} + \sum_{q_1 \neq q_2} (A_{q_1, q_2}^{\parallel} + B_{q_1, q_2}^{\parallel}) \mathcal{Q}''_{q_1, q_2} \quad (46)$$

where  $A_{q_0}^{\parallel\parallel\parallel}$ ,  $A_{q_1, q_2}^{\parallel}$  and  $B_{q_1, q_2}^{\parallel}$  are:

$$A_{q_0}^{\parallel\parallel\parallel} = \left( \frac{2}{N+1} \right)^2 (1 - (-1)^{m_2-m_1}) (1 - (-1)^{m_4-m_3}) \sin^4 \frac{\pi q_0}{N+1} \sum_{p=0}^{\frac{M-(m_4-m_3)-(m_2-m_1)-2}{2}} \left[ \sum_{p_1+p_2+p_3=p} \binom{m_1-1-p_1}{p_1} \binom{m_3-m_2-1-p_2}{p_2} \binom{M-m_4-p_3}{p_3} \right] (2 \cos \frac{\pi q_0}{N+1})^{M-(m_4-m_3)-(m_2-m_1)-2-2p} \quad (47)$$

$$A_{q_1, q_2}^{\parallel} = \left( \frac{2}{N+1} \right)^2 (1 - (-1)^{m_2-m_1}) (1 - (-1)^{m_4-m_3}) \sin^2 \frac{\pi q_1}{N+1} \sin^2 \frac{\pi q_2}{N+1} \left\{ \sum_{p=0}^{\frac{M-(m_2-m_1)-1}{2}} \left[ \sum_{k=0}^p \binom{m_1-1-k}{k} \binom{M-m_2-(p-k)}{p-k} \right] (2 \cos \frac{\pi q_0}{N+1})^{M-(m_2-m_1)-1-2p} \right\} \left\{ \sum_{p=0}^{\frac{M-(m_4-m_3)-1}{2}} \left[ \sum_{k=0}^p \binom{m_3-1-k}{k} \binom{M-m_4-(p-k)}{p-k} \right] (2 \cos \frac{\pi q_0}{N+1})^{M-(m_4-m_3)-1-2p} \right\} \quad (48)$$

$$\begin{aligned}
B_{q_1, q_2}^{\parallel} = & \left( \frac{2}{N+1} \right)^2 (1 - (-1)^{m_3 - m_1}) (1 - (-1)^{m_4 - m_2}) \sin^2 \frac{\pi q_1}{N+1} \sin^2 \frac{\pi q_2}{N+1} \\
& \left\{ \sum_{p=0}^{\frac{M-(m_3-m_1)-1}{2}} \left[ \sum_{k=0}^p \binom{m_1-1-k}{k} \binom{M-m_3-(p-k)}{p-k} \right] (2 \cos \frac{\pi q_0}{N+1})^{M-(m_3-m_1)-1-2p} \right\} \\
& \left\{ \sum_{p=0}^{\frac{M-(m_4-m_2)-1}{2}} \left[ \sum_{k=0}^p \binom{m_2-1-k}{k} \binom{M-m_4-(p-k)}{p-k} \right] (2 \cos \frac{\pi q_0}{N+1})^{M-(m_4-m_2)-1-2p} \right\} \\
& + \left( \frac{2}{N+1} \right)^2 (1 - (-1)^{m_4 - m_1}) (1 - (-1)^{m_3 - m_2}) \sin^2 \frac{\pi q_1}{N+1} \sin^2 \frac{\pi q_2}{N+1} \\
& \left\{ \sum_{p=0}^{\frac{M-(m_4-m_1)-1}{2}} \left[ \sum_{k=0}^p \binom{m_1-1-k}{k} \binom{M-m_4-(p-k)}{p-k} \right] (2 \cos \frac{\pi q_0}{N+1})^{M-(m_4-m_1)-1-2p} \right\} \\
& \left\{ \sum_{p=0}^{\frac{M-(m_3-m_2)-1}{2}} \left[ \sum_{k=0}^p \binom{m_2-1-k}{k} \binom{M-m_3-(p-k)}{p-k} \right] (2 \cos \frac{\pi q_0}{N+1})^{M-(m_3-m_2)-1-2p} \right\}
\end{aligned} \tag{49}$$

For single monomer on the boundary, when  $M$  and  $N$  are both odd:

$$\mathcal{Q}_1 = \sqrt{\frac{2}{N+1}} i^n \sin \frac{\pi \frac{N+1}{2} n}{N+1} i^{\frac{N-1}{2}} \prod_{q=1}^{\frac{N-1}{2}} \left[ \sum_{p=0}^{\frac{M-1}{2}} \binom{M-p}{p} (2 \cos \frac{\pi q}{N+1})^{M-2p} \right] \tag{50}$$

which is zero for  $n$  even and non-zero  $n$ -independent for  $n$  odd, that is

$$\mathcal{Q}_1 = \sqrt{\frac{2}{N+1}} \prod_{q=1}^{\frac{N-1}{2}} \left[ \sum_{p=0}^{\frac{M-1}{2}} \binom{M-p}{p} (2 \cos \frac{\pi q}{N+1})^{M-2p} \right] \tag{51}$$

regardless of the sign or  $i$  factor (which is independent of  $n$  anyway). We can show that (51) is identical with the one in [58] with the aid of the identities (69) and (70).

There are situations where the monomer correlations can obviously be interpreted as dimer ones. In these cases, methods similar to those of the previous section are readily applicable.

## 6 Left-passage probability

Assume boundary conditions such that there exists a chordal path between two vertices on the boundary, in the configurations of the double-dimer model on a  $M \times N$  square lattice. We can do that, for example, by fixing dimers on two adjacent sides of the lattice, alternatively in both underlying dimer configurations. For  $M$  and  $N$  even, this is equivalent to "filling" these sides with monomers and then, inserting one monomer in either dimer configuration, one at the top-left and the other at the bottom-right corner of the remained  $M-1 \times N-1$  square lattice (figure 11). With this "wired/free" boundary conditions, there always be a path from one corner to the other in the double-dimer configurations, and we want to compute the probability of the loop completing this path encompassing any arbitrary face of the lattice, i.e. the left-passage probability. Similar to the previous computation in Sec. 4, we insert the weights  $1 + \epsilon$  and  $1 - \epsilon$ , alternatively on the column of bonds  $\{(M_0 n, M_0 + 1n)\}, n \leq N_0$ , for

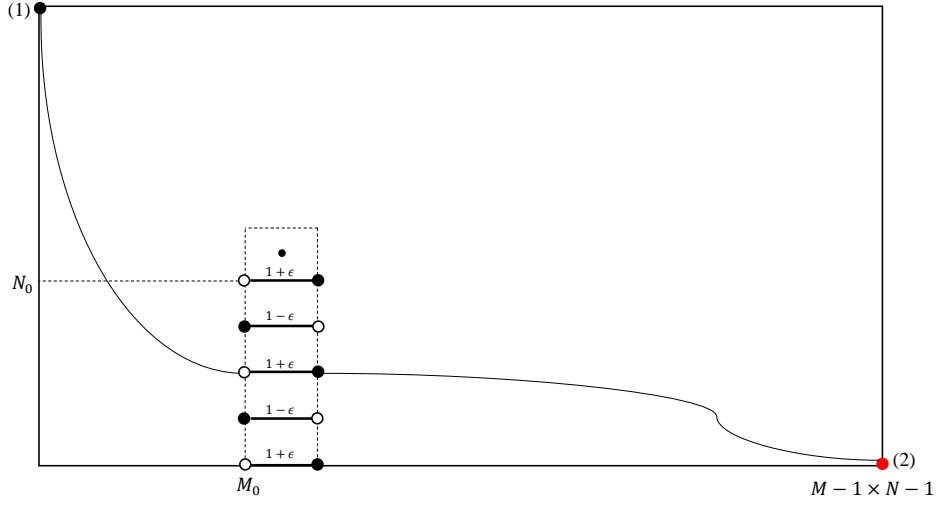


Figure 11: A path due to the insertion of one monomer on the top-left corner in the first dimer model, and another (in red) on the bottom-right corner in the second one.

one dimer model, and likewise for the other replacing  $1 + \epsilon$  by  $1 - \epsilon$ , and vice versa. The actions are

$$\begin{aligned} \mathcal{S}_\epsilon = & \sum_{m=1}^{M-1} \sum_{q=1}^{N-1} \left\{ -c_{m+1q}c_{m-q} - i(-1)^{m+1} \cos \frac{\pi q}{N} c_{mq}c_{m-q} \right\} \\ & - \epsilon \frac{2}{N} \sum_{n=1}^{N_0} \sum_{q,q'=1}^{N-1} c_{M_0+1q}c_{M_0q'} \sin \frac{\pi qn}{N} \sin \frac{\pi q'n}{N} \end{aligned} \quad (52)$$

in the former case and  $\mathcal{S}_{-\epsilon}$  in the latter. We denote by  $\mathcal{Z}_\epsilon$  the partition function of the double-dimer model coming out of the identity  $\mathcal{Z}_\epsilon = \mathcal{Q}_\epsilon^{(1)} \mathcal{Q}_{-\epsilon}^{(2)}$ , where  $\mathcal{Q}_\epsilon^{(1)}$  and  $\mathcal{Q}_{-\epsilon}^{(2)}$  are partition functions of the contributing dimer models, equivalently integrations of the actions  $\mathcal{S}_\epsilon$  and  $\mathcal{S}_{-\epsilon}$  in the presence of one monomer, at the top-left and down-right corner, respectively.

$$\mathcal{Q}_\epsilon^{(1)} = \mathcal{Q}_0^{(1)} + \epsilon C^{(1)} + O(\epsilon^2), \quad \mathcal{Q}_\epsilon^{(2)} = \mathcal{Q}_0^{(2)} + \epsilon C^{(2)} + O(\epsilon^2) \quad (53)$$

and

$$\begin{aligned} \mathcal{Q}_0^{(1)} &= \sqrt{\frac{2}{N}} \prod_{q=1}^{\frac{N-2}{2}} \left[ \sum_{p=0}^{\lfloor \frac{M-1}{2} \rfloor} \binom{M-1-p}{p} (2 \cos \frac{\pi q}{N})^{M-1-2p} \right] \\ &= \mathcal{Q}_0^{(2)} \end{aligned} \quad (54)$$

The coefficient of  $\epsilon$  in the expansion of  $\mathcal{Z}_\epsilon$  is then proportional to the above-mentioned probability for the face  $z = (M_0 + \frac{1}{2}, N_0 + \frac{1}{2})$ , that is

$$\begin{aligned} \mathbb{P}_{\text{left-passage}}(z) &= \text{the coefficient of } \epsilon \text{ in the expansion of } \frac{\mathcal{Q}_\epsilon^{(1)} \mathcal{Q}_\epsilon^{(2)}}{\mathcal{Q}_0^{(1)} \mathcal{Q}_0^{(2)}} \\ &= \frac{C^{(1)} + C^{(2)}}{\mathcal{Q}_0} \end{aligned}$$

where  $\mathcal{Q}_0 = \mathcal{Q}_0^{(1)} = \mathcal{Q}_0^{(2)}$ . The coefficients  $C^{(1)}$  and  $C^{(2)}$  are

$$C^{(1)} = -\frac{2}{N} \left\lfloor \frac{N_0+1}{2} \right\rfloor \mathcal{Q}_0 \delta_{\frac{M_0}{2}, \lfloor \frac{M_0}{2} \rfloor} + \sum_{n=1}^{N_0} \sum_{q_0=1}^{\frac{N-2}{2}} A_{q_0}^{(n)} \mathcal{Q}'_{q_0} + \sum_{n \text{ odd}}^{N_0} \sum_{q_0=1}^{\frac{N-2}{2}} B_{q_0}^{(N-1,n)} \mathcal{Q}'_{q_0}, \quad (55)$$

$$C^{(2)} = -\frac{2}{N} \left\lfloor \frac{N_0 + 1}{2} \right\rfloor \mathcal{Q}_0 \delta_{\frac{M_0-1}{2}, \lfloor \frac{M_0}{2} \rfloor} - \sum_{n=1}^{N_0} \sum_{q_0=1}^{\frac{N-2}{2}} A_{q_0}^{(n)} \mathcal{Q}'_{q_0} + \sum_{n \text{ odd}}^{N_0} \sum_{q_0=1}^{\frac{N-2}{2}} B_{q_0}^{(1,n)} \mathcal{Q}'_{q_0} \quad (56)$$

where  $\mathcal{Q}'_{q_0}$  is defined similarly as before and

$$\begin{aligned} A_{q_0}^{(n)} &= \frac{4}{N} (-1)^{n+1} \sin^2 \frac{\pi q_0 n}{N} \\ &\quad \sum_{p=0}^{\lfloor \frac{M-3}{2} \rfloor} \left[ \sum_{k=0}^p \binom{M_0 - 1 - k}{k} \binom{M - M_0 - 2 - (p - k)}{p - k} \right] (2 \cos \frac{\pi q_0}{N})^{M-3-2p}, \\ B_{q_0}^{(N-1,n)} &= \frac{4}{N} (-1)^{q_0+1} (-1)^{\frac{n-1}{2}} \sin \frac{\pi q_0}{N} \sin \frac{\pi q_0 n}{N} \\ &\quad \sum_{p=0}^{\left\lfloor \frac{M-M_0-2+\delta_{\frac{M_0}{2}, \lfloor \frac{M_0}{2} \rfloor}}{2} \right\rfloor} \binom{M - M_0 - 2 + \delta_{\frac{M_0}{2}, \lfloor \frac{M_0}{2} \rfloor} - p}{p} (2 \cos \frac{\pi q_0}{N})^{M-M_0-2+\delta_{\frac{M_0}{2}, \lfloor \frac{M_0}{2} \rfloor}-2p}, \\ B_{q_0}^{(1,n)} &= \frac{4}{N} (-1)^{\frac{n-1}{2}} \sin \frac{\pi q_0}{N} \sin \frac{\pi q_0 n}{N} \sum_{p=0}^{\left\lfloor \frac{M_0-\delta_{\frac{M_0}{2}, \lfloor \frac{M_0}{2} \rfloor}}{2} \right\rfloor} \binom{M_0 - \delta_{\frac{M_0}{2}, \lfloor \frac{M_0}{2} \rfloor} - p}{p} (2 \cos \frac{\pi q_0}{N})^{M_0-\delta_{\frac{M_0}{2}, \lfloor \frac{M_0}{2} \rfloor}-2p}. \end{aligned}$$

The final result is briefly

$$\mathbb{P}_{\text{left-passage}}(z) = -\frac{2}{N} \left\lfloor \frac{N_0 + 1}{2} \right\rfloor (\delta_{\frac{M_0}{2}, \lfloor \frac{M_0}{2} \rfloor} + \delta_{\frac{M_0-1}{2}, \lfloor \frac{M_0}{2} \rfloor}) + \sum_{n \text{ odd}}^{N_0} \sum_{q_0=1}^{\frac{N-2}{2}} (B_{q_0}^{(N-1,n)} + B_{q_0}^{(1,n)}) \frac{\mathcal{Q}'_{q_0}}{\mathcal{Q}_0} \quad (57)$$

By appropriate arrangements of fugacities, we can compute generalizations of the left-passage probability through similar computations.

Again we are interested in the scaling limit of the above probability (57). Following the approach in Sec. 4, we obtain

$$\mathbb{P}_{\text{left-passage}}(z) \approx \frac{4}{N} \sum_j (-1)^{j+1} \frac{\sin(\frac{N_0 \pi j}{N})}{\sin(\frac{2\pi j}{N})} \frac{\sinh(\frac{(M-M_0)\pi j}{N})}{\sinh(\frac{M\pi j}{N})} + \frac{4}{N} \sum_j \frac{\sin(\frac{N_0 \pi j}{N})}{\sin(\frac{2\pi j}{N})} \frac{\sinh(\frac{M_0 \pi j}{N})}{\sinh(\frac{M\pi j}{N})} - \frac{N_0}{N} \quad (58)$$

where  $j = \frac{N}{2} - q$  and we assume that  $M_0$  is even. Based on the result of [38], we expect (58) to be the harmonic function of  $z$  with boundary values 1 on the top and right sides of any rectangle  $\{0 < x < a, 0 < y < b; \frac{a}{b} = \frac{N}{M}\}$  and zero elsewhere. It is

$$\begin{aligned} u(x, y) &= \sum_{n=1}^{\infty} \frac{-2}{n\pi} \frac{[1 + (-1)^{n+1}]}{\sinh(\frac{n\pi b}{a})} \sin \frac{n\pi x}{a} \sinh \frac{n\pi y}{a} \\ &\quad + \sum_{n=1}^{\infty} \frac{-2}{n\pi} \frac{[1 + (-1)^{n+1}]}{\sinh(\frac{n\pi a}{b})} \sinh \frac{n\pi x}{b} \sin \frac{n\pi y}{b} \end{aligned} \quad (59)$$

In contrast to (59), there is no obvious symmetry with respect to  $M \leftrightarrow N$  and  $M_0 \leftrightarrow N_0$  (equivalently  $a \leftrightarrow b$  and  $x \leftrightarrow y$ ) in (58). To recover such symmetry, we take advantage of complex analysis. If we keep the second term in (58), use the approximation  $\sin(\frac{2\pi j}{N}) \approx \frac{2\pi j}{N}$  and rewrite  $\frac{N_0}{N}$  as  $\frac{N_0}{N} \frac{M-M_0}{M} + \frac{N_0}{N} \frac{M_0}{M}$ , (58) turns out to be (59) by considering the complex-valued functions  $f_1(z) = \frac{\sin(\frac{N_0}{N} z) \sinh(\frac{M-M_0}{N} z)}{z \sin z \sinh(\frac{M}{N} z)}$  and  $f_2(z) = \frac{\sin(\frac{N_0}{N} z) \sinh(\frac{M_0}{N} z)}{z \sin z \sinh(\frac{M}{N} z)}$  and using a result of Cauchy's residue theorem

$$\text{pr.v.} \int_{-\infty}^{\infty} f(x) dx = 2\pi i \sum \text{Res} f(z) + \pi i \sum \text{Res} f(z)$$

where the first sum extends over all poles in the upper half-plane and the second over all simple poles on the real axis. The result of this section is consistent with that of SLE<sub>4</sub> on a rectangle [59].

**Acknowledgments.** We are grateful to Vladimir Plechko for very helpful comments.

## Appendix A Some useful formulas

Here we bring some formulas, referred in the paper. We have used the orthogonality relations

$$\frac{1}{M} \sum_{m=1}^M \exp \left[ i \frac{2\pi(p+p'-1)m}{M} \right] = \delta_{p+p'-1, M}, \quad \frac{1}{M} \sum_{m=1}^M (-1)^m \exp \left[ i \frac{2\pi(p+p'-1)m}{M} \right] = \delta_{p+p'-1, \frac{M}{2}} + \delta_{p+p'-1, \frac{3M}{2}} \quad (60)$$

and

$$\frac{2}{N+1} \sum_{n=1}^N (-1)^{n+1} \sin \frac{\pi q n}{N+1} \sin \frac{\pi q' n}{N+1} = \delta_{q+q', N+1}, \quad \sum_{n=1}^N (\pm 1)^n \sin \frac{\pi q n}{N+1} \cos \frac{\pi q' n}{N+1} = 0 \quad (61)$$

in section 2 in the process of the evaluation of (5), to factorize the partition function.

By using the formula [60]

$$\sum_{k=0}^{\lfloor \frac{n}{2} \rfloor} \binom{n-k}{k} x^k = (-i)^n x^{n/2} U_n \left( \frac{i}{2\sqrt{x}} \right) \quad (62)$$

the partition function (11), for example, can be rewritten as

$$\mathcal{Q}_0 = \prod_{q=1}^{\frac{N}{2}} \left[ (-1)^{M/2} \{ U_M(ix_q) - 4x_q^2 U_{M-2}(ix_q) \} + 2 \right] \quad (N \text{ even}) \quad (63)$$

where  $x_q = \cos \frac{\pi q}{N+1}$ .

We can also use the following [61]

$$\begin{aligned} \prod_{p=1}^{\frac{M}{2}} 2 \left[ \alpha^2 + \sin^2 \frac{\pi(2p-1)}{M} \right]^{\frac{1}{2}} &\equiv \left[ \alpha + (1 + \alpha^2)^{\frac{1}{2}} \right]^{\frac{M}{2}} + \left[ -\alpha + (1 + \alpha^2)^{\frac{1}{2}} \right]^{\frac{M}{2}}, \\ \prod_{p=1}^{\frac{M}{2}} 4 \left[ \alpha^2 + \cos^2 \frac{\pi p}{M+1} \right] &\equiv \frac{\left[ \alpha + (1 + \alpha^2)^{\frac{1}{2}} \right]^{M+1} - \left[ \alpha - (1 + \alpha^2)^{\frac{1}{2}} \right]^{M+1}}{2(1 + \alpha^2)^{\frac{1}{2}}} \end{aligned} \quad (64)$$

valid for even  $M$  and non-negative values of  $\alpha$ , and

$$\sum_{k=0}^{\lfloor \frac{n}{2} \rfloor} \binom{n-k}{k} x^{n-k} = 2^{-n-1} (x+4)^{-\frac{1}{2}} x^{\frac{n}{2}} \left[ (x^{\frac{1}{2}} + (x+4)^{\frac{1}{2}})^{n+1} - (x^{\frac{1}{2}} - (x+4)^{\frac{1}{2}})^{n+1} \right] \quad (65)$$

to check the results for the partition functions in section 2.

The summation formulas

$$\sum_{k=1}^n \cos(kx) = \frac{1}{2} \left[ -1 + \frac{\sin(n + \frac{1}{2})x}{\sin \frac{1}{2}x} \right] \quad (66)$$

,

$$\sum_{k=1}^n (-1)^k \cos(kx) = \frac{1}{2} \left[ -1 + \frac{(-1)^n \cos(n + \frac{1}{2})x}{\cos \frac{1}{2}x} \right] \quad (67)$$

and

$$\sum_{k=1}^{\infty} \frac{\cos(kx)}{k^2 + \alpha^2} = \frac{\pi}{2\alpha} \frac{\cosh \alpha(\pi - x)}{\sinh \alpha\pi} - \frac{1}{2\alpha^2} \quad (68)$$

valid for  $0 \leq x \leq 2\pi$  [62], have been used in section 4 to approximate 34. We have also used the following products in section 5,

$$\prod_{p=1}^{\frac{M-1}{2}} 4 \left[ \alpha^2 + \cos^2 \frac{\pi p}{M+1} \right] \equiv \frac{\left[ \alpha + (1 + \alpha^2)^{\frac{1}{2}} \right]^{M+1} - \left[ \alpha - (1 + \alpha^2)^{\frac{1}{2}} \right]^{M+1}}{4\alpha(1 + \alpha^2)^{\frac{1}{2}}}, \quad (69)$$

$$\prod_{q=1}^{\frac{N-1}{2}} \left[ 2 \cos \left( \frac{\pi q}{N+1} \right) \right] = \sqrt{\frac{N+1}{2}} \quad (70)$$

valid for  $M$  and  $N$  odd [61].

## Appendix B A series formula

One brilliant consequence of contour integration, provided with some conditions, is the Poisson summation formula

$$\sum_{n \in \mathbb{Z}} f(n) = \sum_{n \in \mathbb{Z}} \hat{f}(n) \quad (71)$$

where  $\hat{f}(\xi) = \int_{-\infty}^{\infty} f(x) e^{-2\pi i x \xi} dx$  is the Fourier transform of  $f$ . It is grounded in Cauchy's residue theorem and in turn has many far-reaching consequences in number theory, partial differential equations, statistical studies of time-series, and even improving the computability of slow convergent series [63–65]. Several interesting and practically important identities have been derived from (71), here we derive another one.

**Proposition.** For every  $\alpha \in \mathbb{R}^*$  and  $2m \in \mathbb{Z}^*$ , the following identity holds

$$\sum_{n=-\infty}^{\infty} \frac{1}{\cosh(\alpha n) + \cosh(\alpha m)} = \frac{2m}{\sinh(\alpha m)}. \quad (72)$$

where by  $\mathbb{R}^*$  and  $\mathbb{Z}^*$  we mean  $\mathbb{R} \setminus \{0\}$  and  $\mathbb{Z} \setminus \{0\}$ , respectively.

An application of identity (72) has appeared in section 4, where we have used the summation of odd and even terms separately. We believe this identity is of independent interest and could have general applications.

*Proof.* We consider the function  $f(x) = \frac{1}{\cosh(\alpha x) + \cosh t}$ ,  $t$  a non-zero parameter which is also real at the moment. First, we note that  $f$  can be analytically continued in a horizontal strip containing the real axis, and there exists  $A > 0$  such that  $|f(x)| \leq A/(1 + x^2)$  for all  $x \in \mathbb{R}$ , i.e.  $f$  has moderate decrease at infinity. These conditions are sufficient for the integral defining the Fourier transform to converge [63].

We recall the calculation of Fourier transforms in [63], which in this case obtains  $\hat{f}(\xi) = \frac{2\pi}{\alpha \sinh t} \frac{\sin(\frac{2\pi t}{\alpha} \xi)}{\sinh(\frac{2\pi^2}{\alpha} \xi)}$ .

Applying (71) to  $f$  and  $\hat{f}$  leads to

$$\sum_{n=-\infty}^{\infty} \frac{1}{\cosh(\alpha n) + \cosh t} = \sum_{n=-\infty}^{\infty} \frac{2\pi}{\alpha \sinh t} \frac{\sin(\frac{2\pi t}{\alpha} n)}{\sinh(\frac{2\pi^2}{\alpha} n)}$$

Now, if  $2t/\alpha$  is a non-zero integer number, all the terms on the right-hand side will vanish with the exception of the one for  $n = 0$ , which equals  $\frac{2t/\alpha}{\sinh t}$ . This results in the desired identity.  $\square$

It is interesting that if  $t/\alpha \in \mathbb{Z}^*$ , the odd and even terms of the series (72) have equal contributions in summation. We can easily show that by, for example, the Fourier transform of  $f(x) = \frac{1}{\cosh(2\alpha z) + \cosh t}$  for  $t/\alpha \in \mathbb{Z}^*$ .

**Remark.** Though (72) is exclusively holds for  $m \in \mathbb{Z}^*/2$ , one can check that the RHS of (72) is a very effective approximation for the above-mentioned series if  $|\alpha|$  is not so large (roughly, up to nearly 1 suffices).

## References

- [1] Schramm, O.: *Scaling limits of loop-erased random walks and uniform spanning trees*. Israel J. Math. 118-221 (2000)
- [2] Lawler, G.F., Schramm, O., Werner, W.: *Conformal invariance of planar loop-erased random walks and uniform spanning trees*. Selected Works of Oded Schramm. Springer, New York, NY, 931-987 (2011)
- [3] Rohde, S., Schramm, O.: *Basic properties of SLE*. Selected Works of Oded Schramm. Springer, New York, NY, 989-1030 (2011)
- [4] Smirnov, S.: *Towards conformal invariance of 2D lattice models*. arXiv preprint arXiv:0708.0032 (2007)
- [5] Katori, M.: *Bessel Processes, Schramm-Loewner Evolution, and the Dyson Model*. Springer, Singapore (2015)
- [6] Werner, W.: *The conformally invariant measure on self-avoiding loops*. J. Amer. Math. Soc. 21, 137-169 (2008)
- [7] Sheffield, S.: *Exploration trees and conformal loop ensembles*. Duke Math. J. 147, 79-129 (2009)
- [8] van de Brug, T., Camia, F., Lis, M.: *Random walk loop soups and conformal loop ensembles*. Probab. Theory Related Fields, 166(1-2), 553-584 (2016)
- [9] Werner, W.: *Random planar curves and Schramm-Loewner evolutions*. In *Lectures on probability theory and statistics*, vol. 1840 of Lecture Notes in Math., Springer, Berlin, 107-195 (2004)
- [10] Kager, W., Nienhuis, B.: *A guide to stochastic Loewner evolution and its applications*. J. Stat. Phys. 115, 1149 (2004)
- [11] Rouhani, S.: *Introduction to Schramm-Loewner evolution and its application to critical systems*. Physical Chemistry Research 3.1, 1-15 (2015)
- [12] Smirnov, S.: *Conformal invariance in random cluster models. I. Holomorphic fermions in the Ising model*. Ann. Math. (2) 172, 2, 1435-1467 (2010)
- [13] Chelkak, D., Duminil-Copin, H., Hongler, C., Kemppainen, A., Smirnov, S.: *Convergence of Ising interfaces to Schramm's SLE curves*. C. R. Math. Acad. Sci. Paris, 352(2), 157-161 (2014)
- [14] Saleur, H.: *Lattice models and conformal field theories*. Phys. Rep. 184, 177 (1989)
- [15] Duplantier, B.: *two-dimensional fractal geometry, critical phenomena and conformal invariance*. Phys. Rep. 184, 177 (1989)
- [16] Vanderzande, C.: *Lattice models of polymers*. Cambridge University Press (1998)
- [17] Nienhuis, B.: *Coulomb gas formulation of two-dimensional phase transitions*. in *Phase transitions and critical phenomena*, 11, Domb, C., Lebowitz, J.L., eds. Academic (1987)

- [18] Henkel, M.: *Conformal invariance and critical phenomena*. Texts and Monographs in Physics. Springer-Verlag, Berlin (1999)
- [19] Cardy, J.: *SLE for theoretical physicists*. Ann. Phys. 318, 81 (2005)
- [20] Sheffield, S., Werner, W.: *Conformal loop ensembles: the Markovian characterization and the loop-soup construction*. Ann. Math. 176, 1827-1917 (2012)
- [21] Bauer, M., Bernard, D.: *Conformal transformations and the SLE partition function martingale*. Commun. Math. Phys. 239, 493-521 (2003)
- [22] Friedrich, R., Werner, W.: *Conformal fields, restriction properties, degenerate representations and SLE*. C. R. Math. Acad. Sci. Paris 335, 947 (2002)
- [23] Friedrich, R., Werner, W.: *Conformal restriction, highest-weight representations and SLE*. Comm. Math. Phys. 243, 105122 (2003)
- [24] Schramm, O., Sheffield, S.: *Contour lines of the two-dimensional discrete gaussian free field*. Acta Math. 202(1), 21137 (2009)
- [25] Kenyon, R.: *An introduction to the dimer model*. In School and Conference on Probability Theory, ICTP Lect. Notes, XVII, 267304 (2004)
- [26] Sheffield, S.: *Gaussian free fields for mathematicians*. Probab. Theory Related Fields, 139(3-4), 521541 (2007)
- [27] Kenyon, R.: *The Laplacian and Dirac operators on critical planar graphs*. Invent. Math. 150(2), 409-439 (2002)
- [28] Kardar, M., Parisi, G., Zhang, Y.C.: *Dynamic scaling of growing interfaces*. Phys. Rev. Lett 56, 889892 (1986)
- [29] Borodin, A., Ferrari, P.L.: *Anisotropic growth of random surfaces in 2+1 dimensions*. Comm. Math. Phys. (2013)
- [30] Dubedat, J.: *SLE and the Free Field: Partition functions and couplings*. J. Amer. Math. Soc. 22, 995-1054 (2009)
- [31] Menglu, W., Wu, H.: *Level lines of Gaussian free field I: zero-boundary GFF*. Stochastic Processes and their Applications, 127(4), 1045-1124 (2017)
- [32] Werner, W.: *SLEs as boundaries of clusters of Brownian loops*. C. R. Math. Acad. Sci. Paris, 337(7), 481486 (2003)
- [33] Lawler, G.F., Werner, W.: *The Brownian loop soup*. Probab. Theory Relat. Fields 128, 565-588 (2004)
- [34] Camia, F., Gandolfi, A., Kleban, M.: *Conformal correlation functions in the Brownian loop soup*. Nuclear Physics, Section B, 902, 483-507 (2016)
- [35] Daryaei, E., Araujo, N.A.M., Schrenk, K.J., Rouhani, S., Herrmann, H.J.: *Watersheds are Schramm-Loewner evolution curves*. Physical review letters, 109(21), 218701 (2012)
- [36] Saberi, A.A., Rajabpour, M.A., Rouhani, S.: *Conformal curves on the WO<sub>3</sub> surface*. Physical review letters, 100(4), 044504 (2008)
- [37] Kobayashi, N., Yamazaki, Y., Kuninaka, H., Katori, M., Matsushita, M., Matsushita, S., Chiang, L.Y.: *Fractal Structure of Isothermal Lines and Loops on the Cosmic Microwave Background*. Journal of the Physical Society of Japan, 80(7), 074003 (2011)
- [38] Kenyon, R.: *Conformal invariance of loops in the double-dimer model*. Commun. Math. Phys. 326, 477497 (2014)



- [39] Kenyon, R.: *Dominos and the Gaussian free field*. Ann. Probab., 29(3), 1128-1137 (2001)
- [40] Fowler, R.H., Rushbrooke, G.S.: *An attempt to extend the statistical theory of perfect solutions*. Trans. Faraday Soc. 33, 1272-1294 (1937)
- [41] Kasteleyn, P.W.: *The statistics of dimers on a lattice. I. The number of dimer arrangements on a quadratic lattice*. Physica (Amsterdam) 27, 1209-1225 (1961)
- [42] Temperley, W., Fisher, M.: *Dimer problem in statistical mechanics-an exact result*. Philos. Mag. (8)6, 1061-1063 (1961)
- [43] Wu, F.Y.: *Dimers on two-dimensional lattices*. Internat. J. Modern Phys. B, 20(32), 5357-5371 (2006)
- [44] Cohn, H., Elkies, N., Propp, J.: *Local statistics for random domino tilings of the Aztec diamond*. Duke Math. J. 85, 117-166 (1996)
- [45] Kenyon, R.: *Local statistics of lattice dimers*. Ann. Inst. Henri Poincaré, Probability and statistics, 33, 591-618 (1997)
- [46] Cohn, H., Kenyon, R., Propp, J.: *A variational principle for domino tilings*. J. Amer. Math. Soc., 14, 297-346 (2001)
- [47] Boutillier, C.: *The bead model and limit behaviors of dimer models*. Ann. Probab., 37(1), 107-142 (2009)
- [48] Kasteleyn, P.W.: *Dimer statistics and phase transitions*. J. Math. Phys., 4, 287-293 (1963)
- [49] Fisher, M.E.: *On the dimer solution of planar Ising models*. J. Math. Phys., 7, 1776-1781 (1966)
- [50] Kenyon, R., Miller, J., Sheffield, S., Wilson, D.B.: *Six-vertex model and Schramm-Loewner evolution*. Physical Review E 95(5), 052146 (2017)
- [51] Baxter, R.J.: *Exactly solved models in statistical mechanics*. Academic Press, London (1982)
- [52] Hayn, R., Plechko, V.N.: *Grassmann Variable Analysis for Dimer Problems in Two Dimensions*. J. Phys. A, 27(14), 4753-4760 (1994)
- [53] Allegra, N., Fortin, J.Y.: *Grassmannian representation of the two-dimensional monomer-dimer model*. Physical Review E, 89(6), 062107 (2014)
- [54] Jerrum, M.: *Two-dimensional monomer-dimer systems are computationally intractable*. J. Statist. Phys. 48, 1211-1234 (1987); Erratum in 59, 1087-1088 (1990)
- [55] Valiant, L.G.: *The complexity of computing the permanent*. Theoretical Computer Science, 8(2), 189-201 (1979)
- [56] Plechko, V.N.: *Simple solution of two-dimensional Ising model on a torus in terms of Grassmann integrals*. Theoretical and Mathematical Physics, 64, 748-756 (1985)
- [57] Pinsky, M.A.: *Partial Differential Equations and Boundary-Value Problems with Applications*. Boston, McGraw-Hills (1998)
- [58] Allegra, N.: *Exact solution of the 2d dimer model: Corner free energy, correlation functions and combinatorics*. Nuclear Physics B, 894, 685-732 (2015)
- [59] Schramm, O.: *A percolation formula*. Electronic Communications in Probability, 6, 115-120 (2001)
- [60] Riordan, J.: *Combinatorial Identities*. John Wiley Sons, Inc., New York (1968)
- [61] Chamberland, M.: *Finite trigonometric product and sum identities*. Fibonacci Quarterly 50(3), 217-221 (2012)

- [62] Gradstein, I.S., Ryzhik, I.M.: *Tables of integrals, series, and products*. New York, Academic Press (1980)
- [63] Stein, E.M., Shakarchi, R.: *Complex Analysis*. Princeton University Press (2003)
- [64] Loukas, G.: *Classical and Modern Fourier Analysis*. Pearson Education (2004)
- [65] Melnikov, Y.A., Melnikov, M.Y.: *Computability of series representations for Green's functions in a rectangle*. Engineering Analysis with Boundary Elements, 30, 1 (2006)